



Cite this: *Org. Biomol. Chem.*, 2016, **14**, 5088

Donor/acceptor chromophores-decorated triazolyl unnatural nucleosides: synthesis, photophysical properties and study of interaction with BSA†

Subhendu Sekhar Bag,* Sangita Talukdar, Suman Kalyan Das, Manoj Kumar Pradhan and Soumen Mukherjee

Much effort has been put forth to develop unnatural, stable, hydrophobic base pairs with orthogonal recognition properties and study their effect on DNA duplex stabilisation. Our continuous efforts on the design of fluorescent unnatural biomolecular building blocks lead us to the synthesis of some triazolyl donor/acceptor unnatural nucleosides *via* an azide-alkyne 1,3-dipolar cycloaddition reaction as a key step, which we want to report herein. We have studied their photophysical properties and found interesting solvatochromic fluorescence for two of the nucleosides. Photophysical interactions among two donor-acceptor β -nucleosides as well as a pair of α/β -nucleosides have also been evaluated. Furthermore, we have exploited one of the fluorescent nucleosides in studying its interaction with BSA with the help of UV-visible and steady state fluorescence techniques. Our design concept is based on the hypothesis that a pair of such donor/acceptor nucleosides might be involved in π -stacking as well as in photophysical interactions, leading to stabilization of the DNA duplex if such nucleosides can be incorporated into short oligonucleotide sequences. Therefore, the designed bases may find application in biophysical studies in the context of DNA.

Received 5th March 2016,
Accepted 21st April 2016

DOI: 10.1039/c6ob00500d

www.rsc.org/obc

Introduction

The concept of expanding the genetic alphabet was pioneered with the development of orthogonal base pairing between iso-G and iso-C by Prof. Alex Rich¹ in 1962, with an expectation to generate DNA systems with enhanced functional and informational potential. Inspired by this, Prof. Steven A. Benner in the late 1980s succeeded in expanding the genetic alphabet from four to six letters.^{2*a-i*} Following Benner's work, many researchers have contributed to the field of expansion of the genetic alphabet.³⁻⁵ As a result, a large number of unnatural nucleosides capable of showing H-bonding/ π -stacking interaction properties have been developed and their biophysical properties in the context of DNA have been vigorously investigated.³⁻⁵ Later on in 1994, the creation of non-H-bonding unnatural nucleobase surrogates by Kool *et al.* has

opened a new dimension in the design of hydrophobic unnatural DNA base analogues considering possible aromatic stacking, hydrophobic or CH- π interactions between the base pairs to stabilize DNA duplexes.⁶ Triggered by Kool's work, much effort has been put forth to develop unnatural, stable, hydrophobic base pairs of orthogonal recognition properties towards expanding the genetic alphabet. Scientists are now able to show the expanded informational and functional potential of DNA with the expanded genetic alphabet.⁷ Therefore, not only is the design and synthesis of efficient new base pairs an exciting research area, but also the application of these artificial base pairs to drive the synthesis of unnatural proteins is currently an attractive research field.⁸ Thus, the efforts toward developing a third base pair have mainly focused on the design of nucleobase analogues to pair *via* orthogonal hydrogen bonding, based on the work of the Benner group, and on predominantly non-H-bonding analogues that pair *via* hydrophobic interactions, based on the work of the Kool group. Recent efforts have resulted in the design and construction of a number of such base pairs that includes stable H-bonded pairs⁹ and unnatural, stable, hydrophobic base pairs.¹⁰

However, the rational design of non-hydrogen bonding base pairs remains a challenge. In most of the design of non-hydrogen bonding base pairs, such as C-aryl and/or N-aryl unnatural

Bio-organic Chemistry Laboratory, Department of Chemistry, Indian Institute of Technology Guwahati-781039, India. E-mail: ssbag75@iitg.ernet.in;

Fax: +91-258-2349; Tel: +91-258-2324

† Electronic supplementary information (ESI) available: Photophysical spectra, NMR spectra, and crystallographic data. CCDC 995716 and 995717. For ESI and crystallographic data in CIF or other electronic format see DOI: 10.1039/c6ob00500d

nucleosides, researchers have concentrated mainly on factors like π -stacking, hydrophobicity, steric shape mimicry and in a few cases the dipole moment, *etc.*, in the stabilization of DNA duplexes.^{6–11} However, because of the challenging problem of enzymatic replication of such base pairs, only very few of these artificial base pairs have been efficiently and selectively replicated.

Furthermore, the lack of naturally occurring fluorescent bases has spurred the development of artificial nucleosides with interesting photophysical properties which could be used as probes for DNA analysis, to develop nucleic acid-based diagnostics and sensing materials.^{12,13} As a result of tremendous research efforts, from various scientific corners out of inspiration from nature or a rational designing approach, several unnatural fluorescent nucleobases have been designed for the development of functional nucleic acids, such as nucleic acid-based sensors, DNA-based light harvesting materials and oligonucleotides with novel electronic or magnetic properties.^{14–17} Considering the drawback of structural perturbation caused by extrinsic fluorescent labels, enzymatic replication as well as the application as functional DNA materials, the generation of ideal fluorescent DNA nucleoside base analogues/base surrogates would be much more beneficial. Thus, the field of designing fluorescent nucleoside base analogues of high solvofluorochromicity is flourishing, and many more advancements in the field are expected in the near future. Therefore, the rapidly growing research toward the expansion of the genetic alphabet as well as the growing demand of nucleic acid-based diagnostics and sensing materials necessitates the design of fluorescent unnatural nucleobases with tuned photophysical properties, a pair of which could impart high duplex stability and polymerase replication fidelity.

While in the design of unnatural nucleobases/fluorescent nucleoside base surrogates the concept of H-bonding mimicry or forces like π - π stacking/hydrophobic interactions were the central consideration, forces like charge transfer complexation have not been considered in the context of fluorescent DNA base design or duplex stabilisation. Only recently, Iverson *et al.*¹⁸ have demonstrated that the DNA duplex stability and specificity can be driven by the electrostatic complementarity between an electron-rich and an electron deficient non-nucleosidic base pair. However, interactions among the unnatural donor-acceptor nucleobases *via* charge transfer complexation have not been considered, which might have a potential impact on DNA duplex stabilization.

Our continuous research efforts towards the generation of fluorescent biomolecular building blocks with tuned photophysical properties *via* click reactions¹⁹ has inspired us to think of an alternative force for base pairing which could stabilize the DNA duplex as well as afford fluorescent oligonucleotides with interesting photophysical properties. Thus, inspired by Mulliken's proposal, we took a project for the synthesis of donor-acceptor nucleobases and studied whether the charge transfer complexation (CT) force among a pair of donor-acceptor nucleobases would stabilize the duplex DNA. We ultimately succeeded to show that a donor-acceptor fluorescent triazolyl nucleobase pair formed a CT complex and

afford good stabilization to the duplex DNA. We are the first to introduce the concept of charge transfer-mediated DNA duplex stabilization by a pair of unnatural donor-acceptor triazolyl bases. While the strong duplex stabilization of the self-pair is the result of π - π -stacking interactions, the hetero-pair stabilization has been explained on the basis of charge transfer complexation between the donor and the acceptor bases.²⁰ Moreover, the nucleosides were found to stabilize an abasic site to an extent that is comparable to that of the stability of a natural A-T pair.²¹ Inspired by our first development and result, we thought that it would be worthwhile to synthesize more triazolyl nucleosides containing donor/acceptor aromatics so as to produce a greater number of such exciting pairs with interesting photophysical properties. The basis of our triazolyl nucleoside design was our previous study wherein we showed that the triazolyl units are capable of installing fluorescence properties into a non-fluorescent precursor, as well as electronic coupling between a triazole and a fluorophore giving rise to a modulated emission response to the fluorophore.¹⁹

There exist numerous examples of natural/unnatural nucleosides decorated with the triazole moiety, however in many of the examples, the triazole moiety has been utilized as a linker either to link a fluorophore with the natural bases or as a replacement of the phosphodiester linkage. Moreover, the focus of the synthesis of the few existing triazolyl nucleoside bases wherein the nucleobases were replaced by the triazole units was mainly of synthetic interest or to generate a set of biologically active nucleosides. However, there are no reports of fluorescent triazolyl nucleosides which stabilise DNA duplexes to a good extent.

Inspired by our recent result and in order to generate a new dataset of donor-acceptor triazolyl nucleoside/fluorescent triazolyl base surrogates, we report herein the synthesis and photophysical properties of some triazolyl donor/acceptor nucleosides (Fig. 1). The synthesized new triazolyl nucleosides showed interesting photophysical properties and are expected to stabilize DNA duplexes *via* π -stacking and/or charge transfer interactions if incorporated in DNA in the future. As an application we studied one nucleoside for its interaction with a protein (BSA) biomolecule and found that it could sense proteins with a switch-on fluorescence response with high binding association. Previously, we focused on the synthesis and isolation of only β -nucleosides, however in this report we focus on the synthesis of both α - and β -nucleosides. The exploration of both the α - and β -nucleosides in the DNA context is our future focus.

Results and discussion

Synthesis of unnatural triazolyl donor-acceptor nucleosides

In order to generate a new dataset of nucleoside base surrogates, we report here the synthesis and photophysical properties of some more triazolyl donor/acceptor nucleosides. We have chosen various possible combinations of donor/acceptor aromatics to generate triazolyl donor/acceptor nucleosides with a hope that several donor-acceptor combinations of such

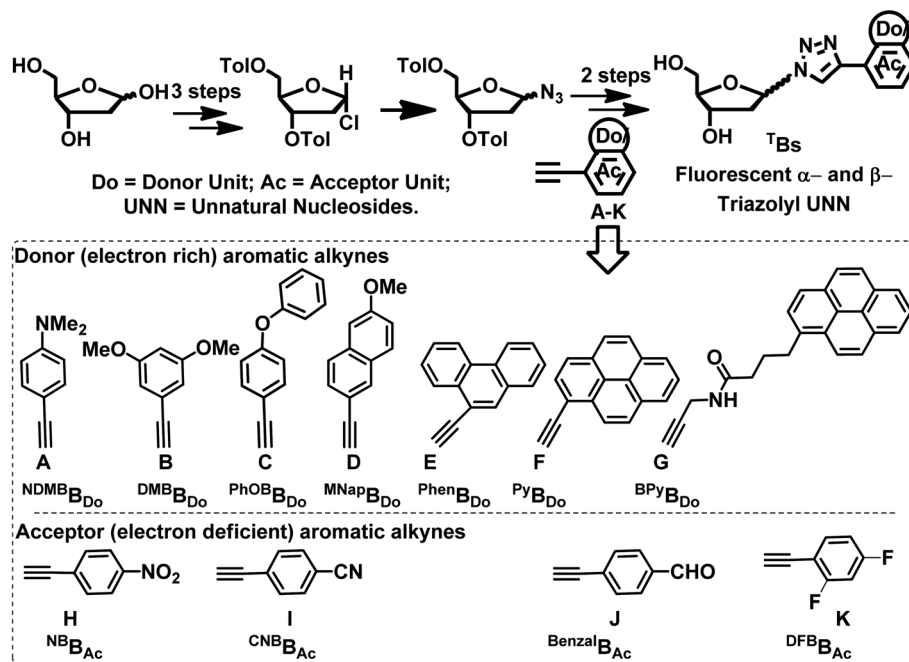
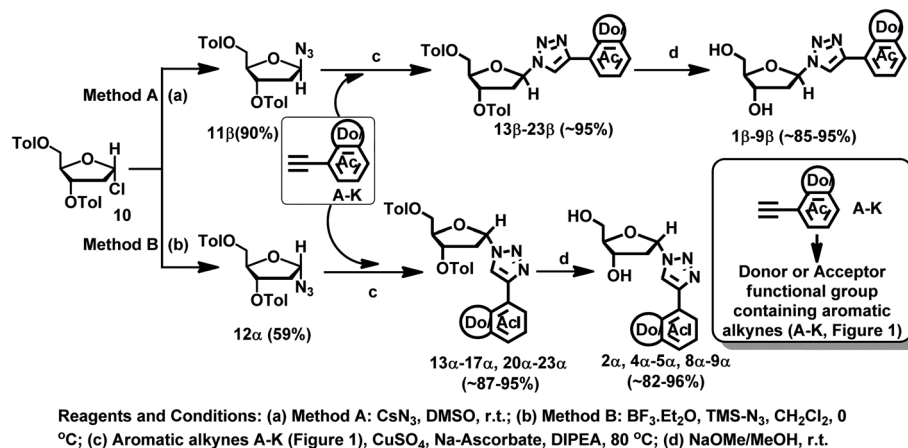


Fig. 1 Schematic presentation for the synthesis of triazolyl unnatural nucleosides (UNN) via a click reaction along with the structures of donor-acceptor alkynes used in the study.

nucleosides might show interesting photophysical properties and afford new pairs of unnatural base pairs for incorporation into DNA, which might stabilize DNA duplexes *via* π -stacking and/or charge transfer interactions. The synthesis of the new class of nucleosides involves the popular 1,3-dipolar azide-alkyne cyclization pathway as a key step in a similar way as we described previously, and is shown in Scheme 1.²⁰

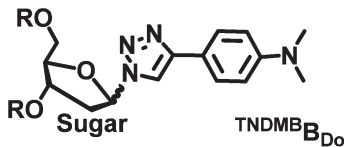
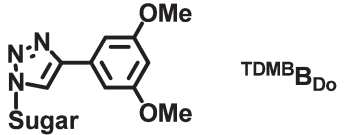
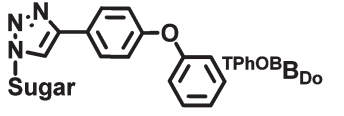
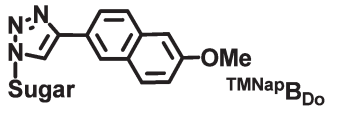
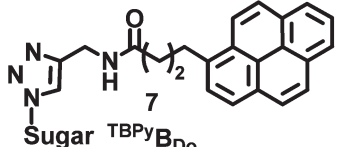
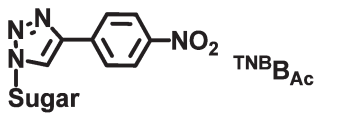
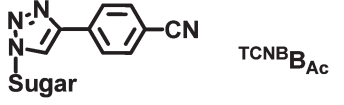
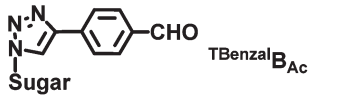
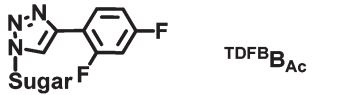
We first synthesized the nucleosides in a similar manner to a procedure we reported previously.^{20,21} Thus, the synthesis started with Hoffer's chlorosugar (10)^{22a} which was synthesised from 2-deoxyribose sugar following our earlier published literature. Hoffer's chlorosugar was then reacted with CsN₃ in DMSO which afforded a 1:10 mixture of α - and β -anomers in excellent yield (Method A), which was utilized for

the synthesis of the β -epimer (11) with 90% yield after purifying by silica gel column chromatography (230–400 mesh) using a hexane:EtOAc solvent system with a gradient of = 30:1 to 20:1. The TMS-N₃ and Lewis acid-mediated protocol (Method B) was adopted to afford the bis-toluoyl-protected α -azidonucleosides (12) in 59% yield starting from Hoffer's chlorosugar (Scheme 1).^{20–23} Our journey of synthesizing several triazolyl nucleosides started from both the α - and β -azides. Thus, both the epimers were reacted separately with various aromatic alkynes (A–K, Fig. 1) containing donor/acceptor substituents in the presence of click reagents at 80 °C in THF to afford triazolyl donor/acceptor nucleosides (13 β –23 β , 13 α –17 α and 20 α –23 α) in the bis-toluoyl protected form in good yields (80–90%, Table 1). Next, methoxide/methanol-



Scheme 1 Synthesis of unnatural donor-acceptor triazolyl α - and β -nucleosides.

Table 1 Alkynes used, short structures of the nucleosides, and yields

Entry	Alkyne	Nucleosides [R = toluoyl or H]	Yield ^a (%)	
			α -Isomer (nucleoside no.)	β -Isomer (nucleoside no.)
1	A	 Sugar TNDMB _{B_{Do}}	87 (13 α) —	97 (13 β) 91 (1 β)
2 ^b	B	 Sugar TDMB _{B_{Do}}	95 (14 α) 95 (2 α)	99 (14 β) 95 (2 β)
3	C	 Sugar TPhOB _{B_{Do}}	52 (15 α) —	90 (15 β) 91 (3 β)
4	D	 Sugar TMNap _{B_{Do}}	98 (16 α) 86 (4 α)	99 (16 β) 88 (4 β)
5 ^b	E	 Sugar TPhen _{B_{Do}}	96 (17 α) 86 (5 α)	95 (17 β) 92 (5 β)
6	F	 Sugar TPy _{B_{Do}}	— —	85 (18 β) 81 (6 β)
7	G	 Sugar TBPpy _{B_{Do}}	— —	95 (19 β) 83 (7 β)
8 ^b	H	 Sugar TNB _{B_{Ac}}	98 (20 α) 82 (8 α)	93 (20 β) 91 (8 β)
9 ^b	I	 Sugar TCNB _{B_{Ac}}	95 (21 α) 94 (9 α)	90 (21 β) 91 (9 β)
10	J	 Sugar TBenzal _{B_{Ac}}	79 (22 α) —	97 (22 β) —
11	K	 Sugar TDFB _{B_{Ac}}	99 (23 α) —	86 (23 β) —

^a Yields in the top row for a particular isomer are for R = toluoyl and for the bottom row are for R = H. ^b See ref. 20 for the β -isomers of entries 2, 5, 8 and 9.

mediated deprotection of the toluoyl groups ultimately afforded the desired α - and β -triazolyl nucleosides (**1 β** –**9 β** , **2 α** , **4 α** –**5 α** and **8 α** –**9 α**) with excellent yields. All the protected and deprotected nucleosides were characterized by NMR, mass spectrometry, IR, melting temperature and in three cases by single crystal X-ray analysis. The α -epimers were synthesized with the aim to incorporate them in future into short oligonucleotide sequences to check the thermal stability of the α -DNA²² as well for the β -DNA context. β -Epimers are the building blocks of natural DNA. Table 1 represents the isolated yields and short structures of the nucleosides. Fig. 2 represents the full structures of all deprotected triazolyl nucleosides.

Structural studies

After getting all the nucleosides in hand we next studied the conformation. The conformation of the β -nucleosides was established *via* NOESY spectra as well as *via* the single crystal X-ray structure of two β -nucleosides, ^{TPhen}B_{Do} (**5 β**) and ^{TNB}B_{Ac} (**8 β**). The NOESY spectra of two representative nucleosides, **5 β** and **9 β** (Fig. 3), showed the presence of cross peaks between H1'–H4', H1'–H2' α , H1'–H_{Triazole} and H_{Triazole}–H_{Aryl}, indicating their β -conformation in solution. The α -conformation of the nucleosides was also established *via* the NOESY spectrum of α -^{TPhen}B_{Do} (**5 α**) as well as *via* the single crystal X-ray structure of α -^{TMNap}B_{Ac} (**4 α**). The NOESY spectrum of the representative α -nucleoside, **5 α** (Fig. 3) showed the presence of cross peaks

between H1'–H2' β , H1'–H_{Triazole} and H_{Triazole}–H_{Aryl} but the absence of a cross peak between H1'–H4' which was present in the β -isomer.

We have recently reported the crystal structure of β -^{TPhen}B_{Do} (**5 β**), which showed an intermolecular π -stacked and H-bonded helical layer network.²⁰ On the other hand, both the packing diagram and crystal arrangement of β -^{TNB}B_{Ac} (**8 β**) show a H-bonded helical layer chain-like structure. Molecules of a single layer are held by H-bonding between sugar CH₂OH...ONO- of nitrobenzene. Another ONO- of one layer is involved in H-bonding with the sugar CH₂OH of the second layer. The two adjacent layers are also involved in stabilized π -stacking interactions between the phenyl ring of a nitrobenzene of one layer and a closely spaced triazole ring of another layer (Fig. 4).

The crystal structure of the β -^{TPhen}B_{Do} (**5 β**) nucleoside shows a twist between the triazole and the phenanthrene, suggesting that the phenanthrene unit might be able to engage in a partial stacking interaction upon incorporation into DNA, which was shown in our earlier report in the context of DNA duplex stabilization in the self-pair duplex containing the β -^{TPhen}B_{Do} (**5 β**) nucleoside.²⁰ However, the nitrobenzene and the triazole moiety of β -^{TNB}B_{Ac} (**8 β**) are in the same plane, which would allow the triazolynitrobenzene unit to take part in intercalation or in a full stacking interaction within the nucleobases inside a DNA duplex after incorporation into

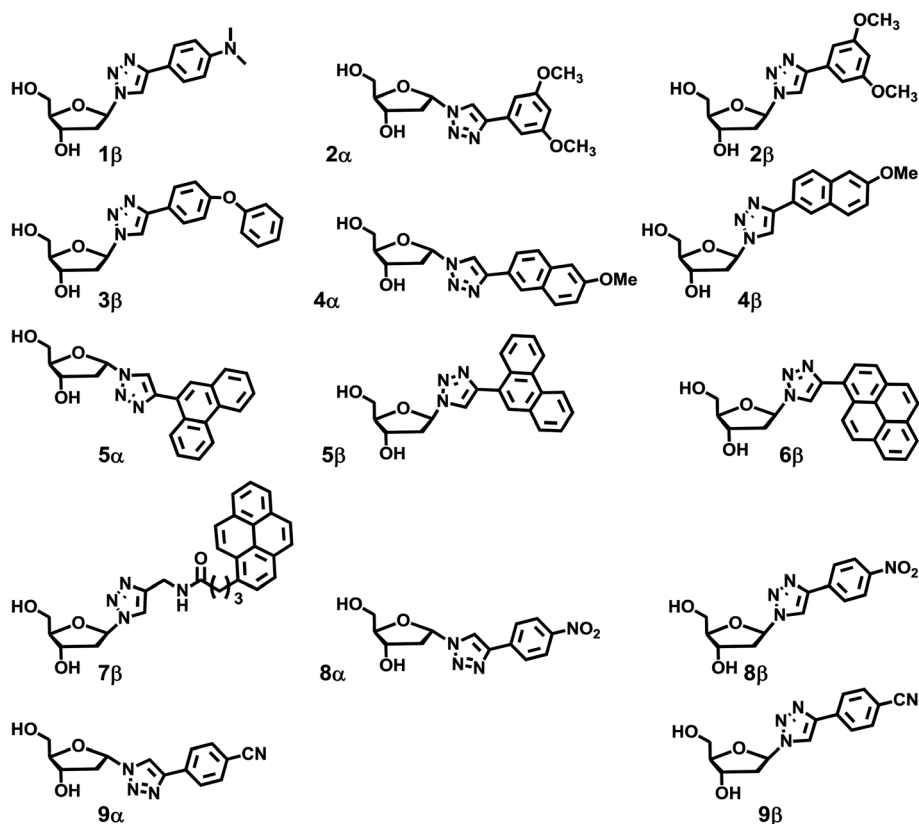


Fig. 2 Structures of the synthesized triazolyl donor/acceptor triazolyl α -/ β -nucleosides.

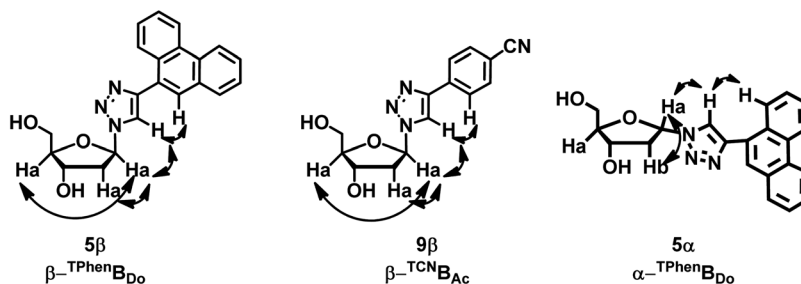


Fig. 3 Presentation of NOESY cross peaks in two representative β -nucleosides and in one α -nucleoside.

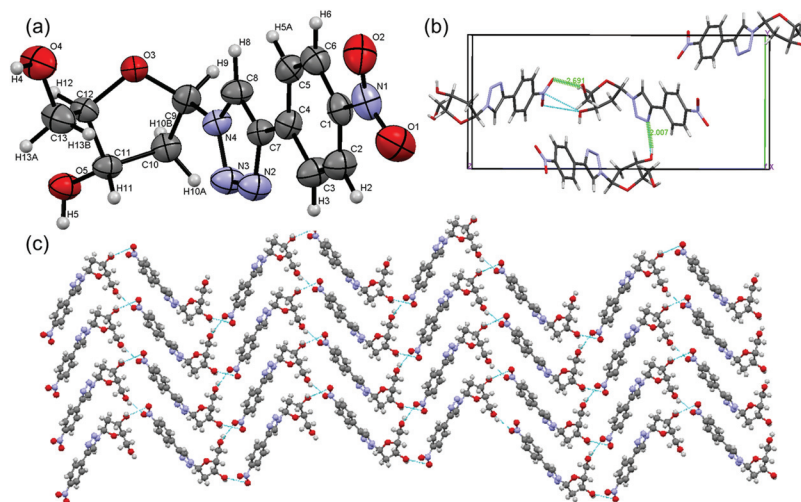


Fig. 4 (a) ORTEP (50% thermal ellipsoid) diagram, (b) crystal packing and (c) π -stacked and H-bonded helical layer network of β - TNBBD_0 (8β) nucleosides [CCDC 995717].

DNA. These all suggested that the triazolyl phenanthrene/nitrobenzene nucleoside can indeed engage in H-bonding as well as π -stacking interactions, and the effect has been shown in the DNA designed in our earlier study.²⁰

The nucleoside α -configuration was also established *via* the single crystal X-ray structure of α - TMNapBD_0 (4α). The crystal packing and arrangements of α - TMNapBD_0 (4α) showed a H-bonded corrugated sheet-like layered structure. The two corrugated planes (each plane containing two layers making a sheet) are held together *via* van der Waals and H-bonding interactions. The first layers of each plane are held by van der Waals (2.387 Å) interactions between the naphthylmethoxy-H of the first plane and the 5'-CH₂-H of the sugar unit of the second plane. Similarly, the second layers of each plane are held by weak H-bonding (2.657 Å) interactions between the naphthylmethoxy-O of the first plane and the 3'-CH-H of the sugar unit of the second plane. Each layer of a plane is held together *via* both intramolecular H-bonding (2.030 Å, between the triazolyl N₂- and the 3'-OH-H) and intermolecular H-bonding (2.714 Å, between the triazolyl 3'-OH and the 5'-OH of sugar units). The two layers of a plane are held *via* π - π stacking interactions in a T-shaped fashion between two aromatic units of each layer *via* aromatic CH- π -interactions and weak

H-bonding interactions (2.836 Å and 2.826 Å, respectively) between the 2'-OH of the sugar of one layer and the pyranose ring -O- of the sugar of the second layer. Interestingly, each plane runs anti-parallel with respect to the pyranose sugar unit. Most importantly, the crystal arrangement follows unidirectional growth along the *c*-axis (Fig. 5).

Study of photophysical properties

After getting all the nucleosides in hand, we studied their UV-visible and fluorescence photophysical properties. Previously we and subsequently others have shown that the linking of fluorescent/non-fluorescent units with a triazole moiety can lead to the installation of fluorescence emission properties to the non-fluorescent molecules and/or modulation of the properties of a fluorescent molecule.¹⁹ The synthesized nucleic acid building blocks (2'-deoxyribosides) also behaved in a similar way with respect to their photophysical properties. We studied the photophysical properties of a few of our synthesized β -nucleosides in various solvents. The nucleoside 1β (TNDMBBD_0) containing a *N,N*-dimethylaminobenzene group exhibits very strong absorption maxima at around 270–280 nm in various organic solvents with ~ 5 nm solvatochromicity. Excitation at the absorption maximum of each solvent shows

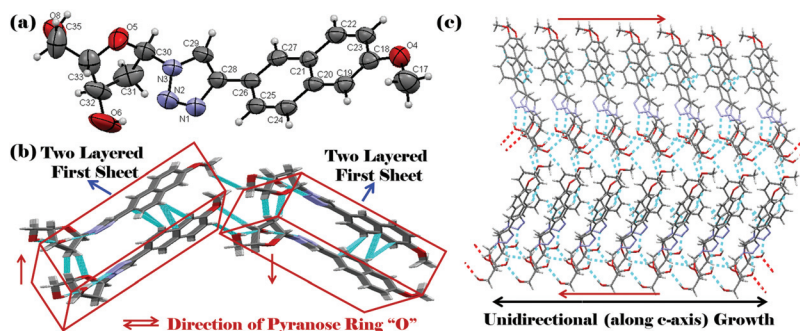


Fig. 5 (a) ORTEP (taking one molecule and 50% thermal ellipsoid) diagram, (b) crystal packing and various interactions and (c) π -stacked and H-bonded corrugated sheet-like network of α - TMNaPBD_0 (4α) nucleosides [CCDC 995716].

an emission at around 365 nm with a red-shift of 10 nm as the solvent polarity increases. While the nucleoside exhibits a long wavelength emission, most probably an intramolecular charge transfer (ICT)^{24,25} band at 485 nm in polar solvents like DMF, DMSO and in acetonitrile, the fluorescence intensity becomes negligible in polar protic solvents like EtOH and MeOH. The quenched incidence of fluorescence can be attributed to the H-bonding-mediated radiationless decay of the chromophore in polar protic solvents (Fig. 6a and b).²⁶ The nucleoside 2β (TDMB_{D_0}) containing a 3,5-dimethoxybenzene group exhibits a very strong absorption maximum at around 252–270 nm and a weak band at around 290 nm in various organic solvents. Excitation at the absorption maximum of each solvent shows emission at around 320 nm with an irregular trend in the intensity as the solvent polarity increases (Fig. 6c and d).

The nucleoside 3β ($\text{TPhOB}_{\text{D}_0}$), which is a phenoxyphenyl-triazole nucleobase, possesses a structureless absorption maximum at around 257–260 nm with little or no solvatochromicity or change in absorbance in all organic solvents tested. Excitation at the absorption maximum of each solvent

shows a structureless emission at around 333 nm with a quenched incidence of fluorescence as the polarity of the solvent increases (Fig. 7a and b).

The nucleoside 4β (TMNaPBD_0) containing a methoxynaphthalene aromatic unit exhibits very strong absorption with vibronic structures at 285, 290 and 302 nm in the least polar solvent, toluene. The absorbance is characterized by a hypsochromic shift (2–5 nm) and little hyperchromism as the polarity of the solvent increases. Excitation at the absorption maximum (290–300 nm) of each solvent shows an emission at around 365 nm with an increase in the intensity as the solvent polarity increases (Fig. 7c and d).

The $\text{TPhen}_{\text{D}_0}$ (5β) nucleoside shows blue-shifted absorbance as the polarity of the solvent increases ($\lambda_{\text{max}} = 302$ nm in dioxane \rightarrow 298 nm in MeOH). Upon excitation at 300 nm, $\text{TPhen}_{\text{D}_0}$ shows structured bands at 363 and 380 nm with similar intensities and low quantum yields in all solvents.²⁰ The triazolylpyrene nucleoside 6β (TPy_{D_0}) shows structureless absorption at 355 nm in toluene which is blue-shifted to

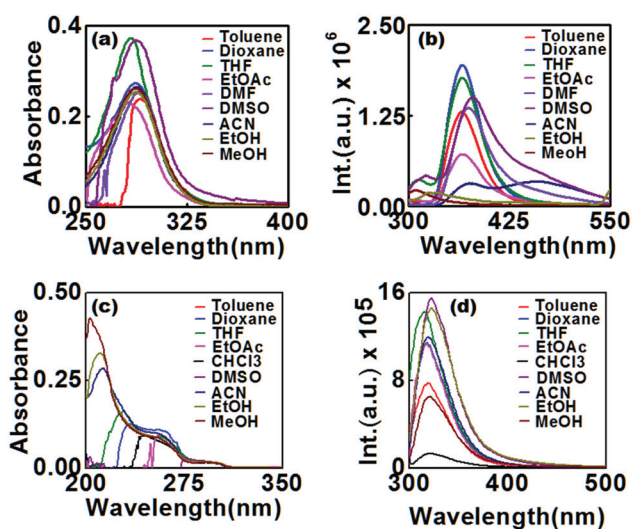


Fig. 6 UV-visible and fluorescence spectra of nucleoside 1β (a–b) and nucleoside 2β (c–d) in various organic solvents (concentration of each nucleoside was 10 μM).

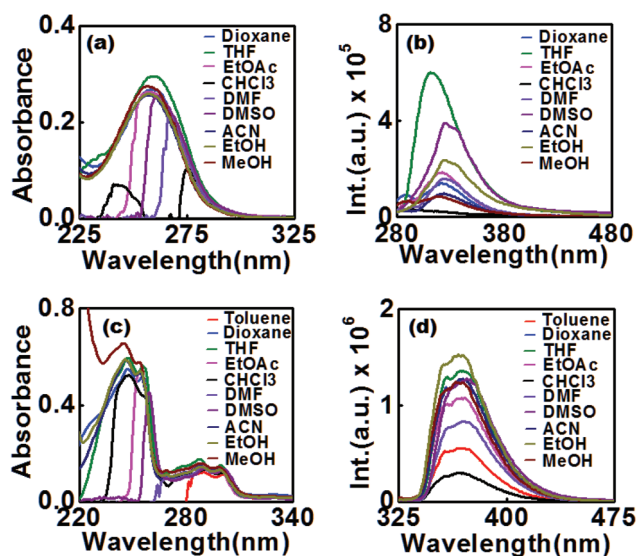


Fig. 7 UV-visible and fluorescence spectra of nucleoside 3β (a–b) and nucleoside 4β (c–d) in various organic solvents (concentration of each nucleoside was 10 μM).

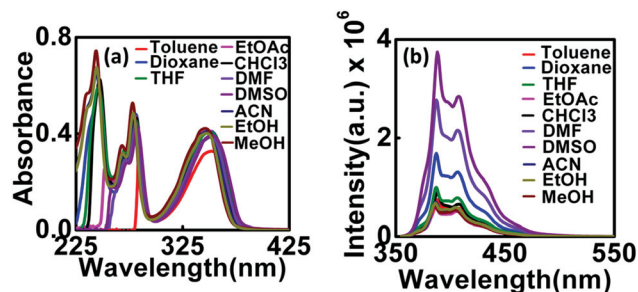


Fig. 8 (a) UV-visible and (b) fluorescence spectra of nucleoside **6β** in various organic solvents (concentration of each nucleoside was 10 μM).

348 nm with the increase in absorbance as the solvent polarity increases, showing an electronic coupling of the pyrenyl π -electron cloud with the triazole unit. However, it shows a structured emission when excited at 350 nm with the appearance of prominent maxima at 387 and 408 nm of similar intensities and quantum yields as the polarity of the solvent increases (Fig. 8a, b and Table 2). The fluorescence life time data also supports this observation (see ESI, Table S4†). On the other hand, the nucleoside **7β** (^{TBPy}B_{Do}) containing a butylpyrene triazole exhibits very strong absorption with vibronic structures characteristic of butylpyrene at 314, 329 and 346 nm in all solvents tested. The absorbance is characterized by a hypsochromic shift (2–5 nm) and little hyperchromism as the polarity of the solvent increases. Excitation at the absorption maximum (~350 nm) in each solvent shows structured emissions at 380, 401, and 421 nm with an increase in intensity as the solvent polarity increases. The fluorescence life time data also supports this observation (Fig. 9a, b and Table 2).

The nucleoside **9β** (^{TCNB}B_{Ac}) containing a cyanobenzene acceptor aromatic unit possesses a very strong structureless absorption at 287 nm in the least polar solvent, toluene.²⁰ The

Table 2 Summary of the photophysical properties of nucleosides **6β** and **7β**

Entry	Solvent	UV-vis. and fluorescence properties			
		λ_{abs} (nm)	$\epsilon_{\text{max}} \times 10^3$	λ_{fl} (nm)	Φ_{f}
^{TBPy} B _{Do} (6β)	Toluene	353	32.6	408	0.13
	Dioxane	351	41.0	407	0.22
	THF	351	40.7	407	0.13
	EtOAc	349	41.2	407	0.08
	CHCl ₃	351	38.6	407	0.12
	DMF	351	38.7	407	0.39
	DMSO	351	39.1	408	0.58
	ACN	348	40.8	406	0.09
	EtOH	347	39.6	406	0.10
	MeOH	346	40.8	405	0.09
^{TBPy} B _{Do} (7β)	Toluene	345	34.2	417	0.07
	THF	344	45.2	417	0.09
	EtOAc	343	42.7	417	0.06
	CHCl ₃	345	38.8	417	0.08
	ACN	343	40.3	417	0.07
	EtOH	342	45.6	417	0.08
	MeOH	342	41.3	417	0.08

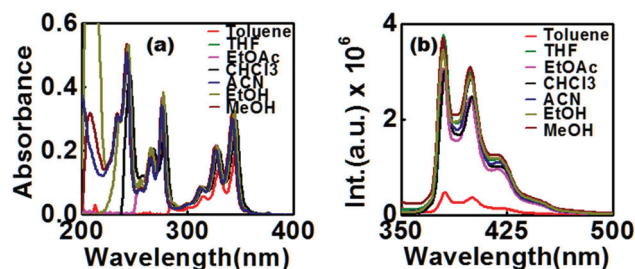


Fig. 9 (a) UV-visible and (b) fluorescence spectra of nucleoside **7β** in various organic solvents (concentration of each nucleoside was 10 μM).

absorbance is characterized by a hypsochromic shift (2–5 nm) and hyperchromism as the polarity of the solvent increases. Excitation at 280 nm shows an emission at around 315 nm in toluene which becomes broad with an appearance of a red-shifted hump (at 335 nm in EtOAc → 353 nm in MeOH) of increased intensity as the solvent polarity increases. This broadened band is most probably the ICT emission. In summary all the triazolyl aromatic nucleosides show significantly red-shifted absorption and emission properties from those of the parent aromatics. It is also obvious that the emission intensity, wavelength and quantum yields are higher than any of the natural nucleosides.²⁰

As representative examples, we have also studied the photo-physical properties, in various organic solvents, of two representative α -triazolyl nucleosides, namely, **4α** and **9α** (Fig. 10a–b and c–d, respectively). Thus, the UV-visible spectra of the α -^{TMN}apB_{Do} (**4α**) nucleoside shows a slightly blue-shifted (3–4 nm) absorbance for all the vibronic bands at 284, 290 and 300 nm as the polarity of the solvent increases (Fig. 10a), which is similar to the corresponding β -anomer, the **4β**-nucleo-

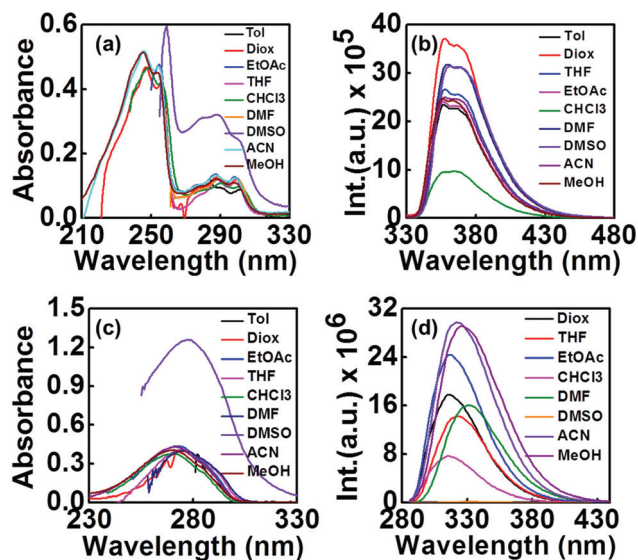


Fig. 10 UV-visible and fluorescence spectra of nucleosides **4α** (a–b) and **9α** (c–d) in various organic solvents (concentration of each nucleoside was 10 μM).

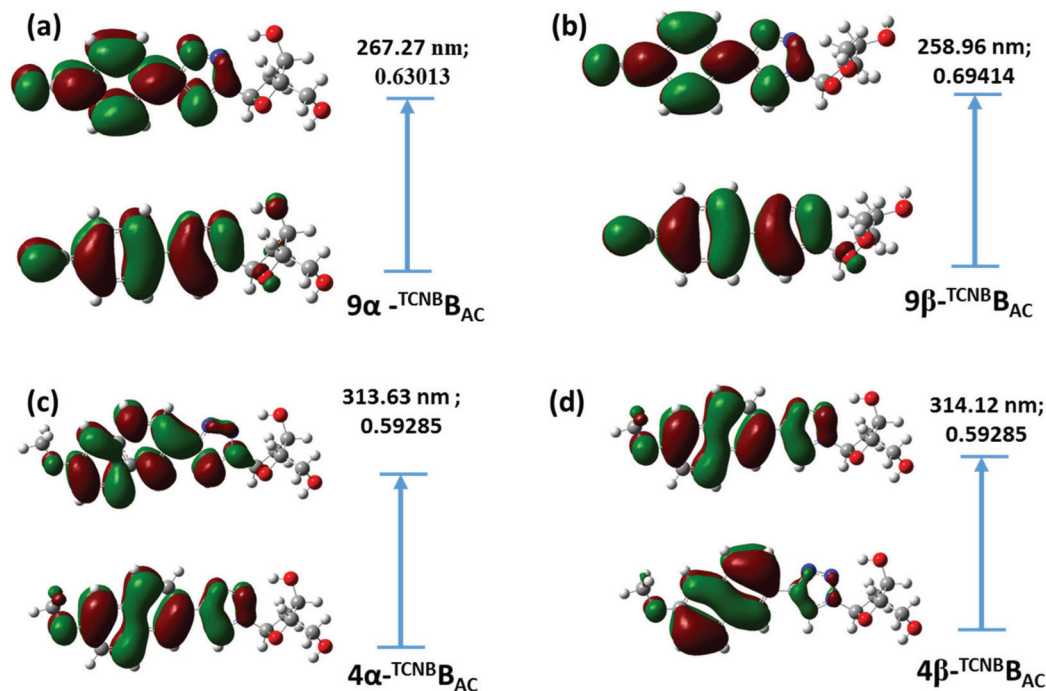


Fig. 11 Diagram of the HOMO–LUMO of nucleosides 4α , 4β , 9α and 9β calculated at the B3LYP//6-31G* level of theory using the Gaussian 03 program package.

side. Surprisingly, the change in both the absorbance and wavelength in the highest aprotic polar solvent, DMSO, is found to be more drastic for 4α compared to 4β . An examination of the emission spectra of 4α reveals the opposite vibronic structure to that of 4β in all the solvents tested. However, the relative intensities of the emissions at 357, 368 nm of the 4α -nucleoside remains almost similar to that observed for the 4β anomer when excited at 300 nm (Fig. 10b). On the other hand, the nucleoside α - $^{\text{TCNB}}\text{B}_{\text{Do}}$ (9α) shows similar absorption behavior to 9β with more or less similar but slight solvatochromicity. On excitation at 280 nm, the nucleoside 9α shows a broad emission band at around 316 nm in toluene, similar to the corresponding 9β -anomer. As the solvent polarity increases the spectral feature becomes broader and shifts to a longer wavelength region. In MeOH the emission band of 9α appears at 327 nm with maximum intensity (Fig. 10c and d) indicating a similar fluorophoric nature as that of the 9β -anomer. Thus, both the α - and β -anomers behave similarly with respect to their photophysical properties.

Theoretical calculation

Next, the absorption and emission properties of four representative donor/acceptor aromatic triazolyl nucleosides ($4\alpha/4\beta$ and $9\alpha/9\beta$) were studied theoretically (TDDFT calculation) using the Gaussian 03 program package.²⁷ The calculations show that the electronic transition from S_0 to S_1 or other possible electronic transitions are feasible, as is revealed from the HOMO–LUMO overlap and the transition oscillator strength (f). This indicates that the reverse transition, *i.e.*, $S_0 \leftarrow S_1$, is also fully allowed, suggesting the fluorophoric nature of all

four triazolyl unnatural nucleosides. The redistribution of electronic charge density between HOMO–LUMO supports the observed emission properties of the fluorophores (Fig. 11).²⁸

For example, the TDDFT calculations show the dominant transition $S_0 \rightarrow S_1$ (HOMO \rightarrow LUMO) in the lowest-lying singlet excited state of both the donor and acceptor triazolyl α/β -nucleosides. The prominent transition is found to be at 270 nm (4.59 eV; HOMO \rightarrow LUMO) with $f = 0.78$ and CI = 0.69 for 4β , and for 4α the transitions occur at 267 nm (4.6389 eV; HOMO \rightarrow LUMO and HOMO–1 \rightarrow LUMO) with $f = 0.75$ and CI = 0.63013 and 0.11, respectively. Similarly, for $9\alpha/9\beta$ the prominent transition is found to be at 313–314 nm, $f = 0.12$, CI = 0.6 (3.95 eV; HOMO \rightarrow LUMO). While the transitions HOMO–1 \rightarrow LUMO (293 nm, 4.22 eV, $f = 0.08$, CI = 0.45) from the second, HOMO \rightarrow LUMO+1 (273 nm, 4.53 eV, $f = 0.04$, CI = 0.56) from the third and HOMO–1 \rightarrow LUMO (247 nm, 5.03 eV, $f = 1.11$, CI = 0.43) from the fourth singlet excited states are also found for 9α , the 9β -nucleoside shows the transitions HOMO \rightarrow LUMO+1 (291 nm, 4.25 eV, $f = 0.10$, CI = 0.46) from the second, HOMO \rightarrow LUMO+2 (262 nm, 4.72 eV, $f = 0.02$, CI = 0.68) from the third and HOMO \rightarrow LUMO+1 (246 nm, 5.03 eV, $f = 1.25$, CI = 0.40) from the fourth singlet excited state. The transitions in the gas phase are in close agreement with the experimental results of 287, 301 nm (in toluene) for 4α , 285, 290 and 302 (in toluene) for 4β , 272, 292 nm (in dioxane) for 9α and 287 nm (in toluene) for 9β .

The emission spectra of the donor–acceptor triazolyl unnatural nucleosides 4α , 4β , 9α and 9β show a slight solvatochromic effect which is due to electronic charge redistribution between the triazole moiety and the fluorophoric unit which is

also reflected from their individual HOMO–LUMO diagrams (Fig. 11). The emissive states are characterized by more significant electron redistribution, *i.e.*, ICT feature, as is suggested by the HOMO–LUMO distributions.²⁸

Study of photophysical interaction

Next, the possible photophysical interaction properties among the Do/Ac nucleoside pairs have been evaluated in different solvents. For this purpose, we have chosen two triazolopyrene nucleosides **6β** and **7β** as donor nucleosides and the triazolopyrene nucleoside **9β** as the acceptor nucleoside. We first have examined the interaction of the donor nucleoside **6β** with an increasing concentration of acceptor nucleoside **9β** in dioxane by recording the UV-visible and fluorescence spectra. Thus, titration of a solution of the triazolopyrene nucleoside (**6β**, 10 μM) in 1,4-dioxane with an increasing concentration of triazolopyrene nucleoside **9β** shows an isosbestic point at 305 nm in the UV-visible spectra, indicating that the two nucleosides are in equilibrium. The mixture shows absorptions with vibronic maxima at 247 nm and 280 nm wherein the absorption of triazolopyrene is buried, and a structureless absorption band at 351 nm that is due to triazolopyrene absorption. With increasing the concentration of the acceptor nucleoside **9β**, the extinction coefficient of the absorption maxima at 247 and 280 nm are increased while the absorption at 351 nm is decreased with very little blue-shift (Fig. 8).

The fluorescence excitation spectra (superimposable to the absorption spectra of the monomer) monitored at 386 nm also shows an isosbestic point at 291 nm with three maxima at 248, 281 and 353 nm. The band at 353 nm shows a decreased intensity along with a little blue-shift indicating that the donor–acceptor nucleosides interact with each other. When excited at the pyrene absorption maximum ($\lambda_{\text{ex}} = 350$ nm) we found no change in either the emission intensity or the wavelength. However, the emission spectra ($\lambda_{\text{em}} = 280$ nm) of the mixture generate two main emission bands at 320 nm characteristic of triazolopyrene and at 406 nm corresponding to the emission of triazolopyrene with an isosbestic point at 370 nm. The decreased intensity of the emission band at 406 nm indicates the quenching of the fluorescence of triazolopyrene by the increased concentration of triazolopyrene (Fig. 12 and ESI, Table S5†).

On the other hand, the titration of a solution of butylpyrenyltriazolyl nucleoside (**7β**, 10 μM) in 1,4-dioxane with increasing concentration of the triazolopyrene nucleoside (**9β**) shows isosbestic points at 247 and 307 nm in the UV-visible spectra, indicating that the two nucleosides are in equilibrium. The mixture shows absorptions with vibronic maxima at 244 nm and 278 nm wherein the absorption of triazolopyrene is buried, and a structureless absorption band at 344 nm along with small bands at 312 and 323 nm that are due to triazolopyrene absorption. With increasing the concentration of the acceptor nucleoside **9β**, the extinction coefficients of the absorption maxima at 244 and 278 nm are found to be increased, while the absorption at 344 nm is decreased

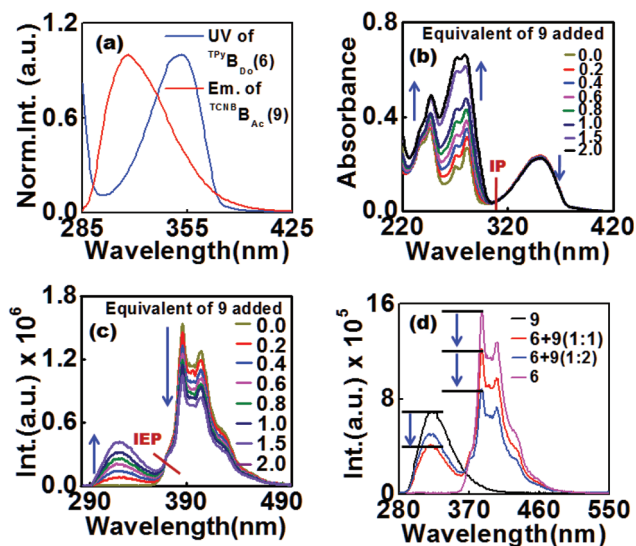


Fig. 12 (a) UV-visible and fluorescence spectra of the triazolopyrene nucleoside, TPyB_{Do} (**6β**, 10 μM) and triazolopyrene nucleoside, TCNB_{Ac} (**9β**, 10 μM) in dioxane. (b–c) UV-visible and fluorescence titration spectra of a solution of **6β** (10 μM) in 1,4-dioxane with an increasing concentration of nucleoside **9β**. (d) Change in the emission intensity of triazolopyrene upon addition of the acceptor nucleoside triazolopyrene nucleoside indicating a quenching of fluorescence incidence.

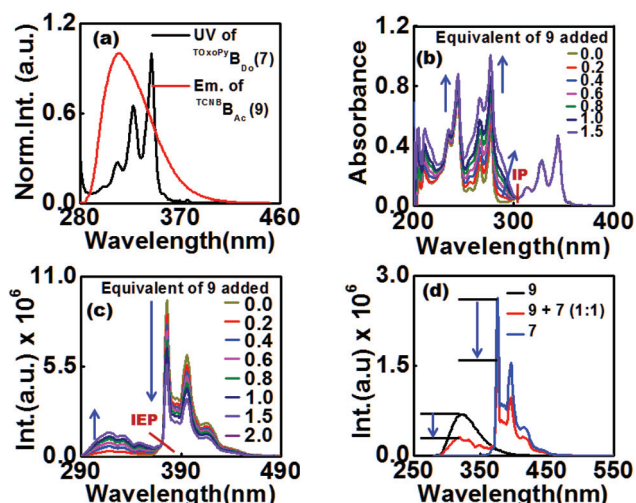


Fig. 13 (a) UV-visible and fluorescence spectra of nucleosides TPyB_{Do} (**7β**, 10 μM) and TCNB_{Ac} (**9β**, 10 μM) in dioxane. (b–c) UV-visible and fluorescence titration spectra of a solution of **7β** (10 μM) in 1,4-dioxane with an increasing concentration of nucleoside **9β**. (d) Change in the emission intensity of triazolopyrene upon addition of the acceptor nucleoside triazolopyrene nucleoside.

with a very small blue-shift (2 nm). A peak at 290 nm also appears, which is the characteristic band of the triazolopyrene nucleoside (Fig. 13).

The fluorescence excitation spectra (superimposable to the absorption spectra of the monomer) monitored at 386 nm also show an isosbestic point at 299 nm with three maxima at 245, 277 and 344 nm. The band at 344 nm shows a decreased

intensity along with a little blue-shift, indicating that the two donor–acceptor nucleosides interact with each other. The emission spectra ($\lambda_{\text{ex}} = 275$ nm) of the mixture features two main emission bands at around 319 nm, characteristic of triazolylcyanobenzene, and at 386 nm, along with other structured bands at 376, 413 and 444 nm corresponding to the emission of the butylpyrenyltriazolyl nucleoside with an isosbestic point at 372 nm. The decreased intensity of the emission band at 376/386 nm indicates the quenching of the fluorescence of butylpyrenyltriazole by the increased concentration of triazolylcyanobenzene (Fig. 13 and ESI, Table S5†).

A closer look at the UV-visible spectra of the nucleoside **6 β** and/or **7 β** and the fluorescence emission spectra of nucleoside **9 β** indicates that there might be a possibility of a FRET process occurring between the donor–acceptor nucleoside pairs leading to quenching of the fluorescence (Fig. 12a and 13a).²⁹ We have calculated the Stern–Volmer quenching constant for each pair of donor–acceptor nucleosides from the slope of the plot of F_0/F vs. conc. of the quencher, which is found to be 5×10^{-2} for the **6 β /9 β** pair and 3.3×10^{-2} for the **7 β /9 β** pair (see ESI, Table S5†). However, at this stage we are unable to conclude the exact mechanism of fluorescence quenching and it needs further investigation. Moreover, excitation at the absorption maxima of either nucleoside **6 β** or **7 β** does not change the fluorescence intensity of the pyrenyl fluorescence in both cases, even with increasing the concentration of the donor nucleoside **9 β** . Surprisingly, decreased fluorescence of triazolylcyanobenzene has been observed upon increasing the concentration of triazolylpyrenyl nucleosides **6 β** or **7 β** when excited at 280 nm (absorption of triazolylcyanobenzene) indicating non-FRET quenching of the fluorescence of the nucleoside **9 β** by **6 β** and/or **7 β** , wherein the nucleosides **6 β** and **7 β** , containing pyrenyltriazole and butylpyrenyltriazole respectively, act as quenchers of triazolylcyanobenzene (see ESI, Fig. S1–2a†). This reverse quenching is most probably because of an electron transfer process from pyrenyltriazole and/or butylpyrenyltriazole to the acceptor cyanobenzene unit of the nucleoside **9 β** .

Similarly, a titration experiment has been carried out between a representative α -acceptor nucleoside, α -TCNB B_{Ac} (**9 α**) and the same β -donor nucleoside, $^{T\text{BPy}}B_{\text{Do}}$ (**7 β**), to examine the possible photophysical interaction properties, if any, in dioxane. We, thus, have titrated a solution of the donor nucleoside **7 β** with an increasing concentration of the acceptor nucleoside **9 α** in dioxane by recording the UV-visible and fluorescence spectra. The UV-visible titration spectra show an isosbestic point at around 307 nm indicating that the two interacting nucleosides are in equilibrium. The mixture shows increasing absorptions of the vibronic maxima at 245, 264, 275 and 285 nm wherein the absorption of triazolylcyanobenzene is buried, and unchanged vibronic absorption bands corresponding to triazolylpyrene at 310, 325 and 344 nm. The absorption band of triazolylcyanobenzene also appears with increasing absorptivity at 288–292 as the concentration of **9 α** increases (Fig. 14a). Thus, the UV-visible titrations indicate a similar result to the titration experiment between **7 β** and **9 β** .

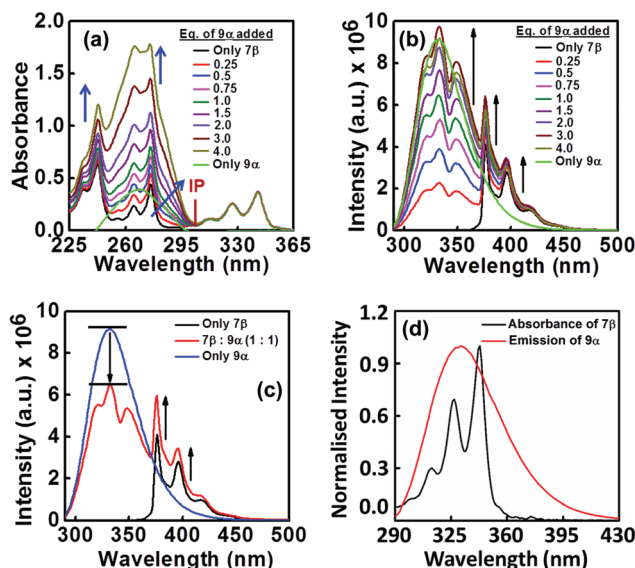


Fig. 14 (a–b) UV-visible and fluorescence titration spectra of a solution of **7 β** (10 μM) in 1,4-dioxane with an increasing concentration of nucleoside **9 α** . (c) Change in the emission intensity of the pyrene of $^{T\text{BPy}}B_{\text{Do}}$ (**7 β**) upon addition of the acceptor nucleoside α -TCNB B_{Ac} (**9 α**). (d) Overlap of the UV-visible and fluorescence spectra of the nucleosides $^{T\text{BPy}}B_{\text{Do}}$ (**7 β** , 10 μM) and α -TCNB B_{Ac} (**9 α** , 10 μM), respectively, in dioxane, showing a possibility of FRET.

The fluorescence excitation spectra monitored at 386 nm show an isosbestic point at 280 nm with decreased intensities of the bands at 241, 264 and 275 nm, and an obviously increased intensity of the buried triazolylcyanobenzene band at around 285 nm. Interestingly an increase in the intensity of all the vibronic bands of pyrene is observed as the concentration of **9 α** increases, which is contrary to the titration between **7 β** and **9 β** wherein the opposite result is observed. This observation indicates a strong interaction among the **9 α /7 β** donor–acceptor nucleosides. The emission spectra ($\lambda_{\text{ex}} = 280$ nm) of the mixture show two main structured emission bands at around 325 nm characteristic of triazolylcyanobenzene and centered at 405 nm corresponding to the emission of the butylpyrenyltriazolyl nucleoside (Fig. 14b). A closer look at the emission spectra of only **7 β** and **9 α** and their 1 : 1 mixture reveals a decrease in the intensity of **9 α** and an increase in the intensity of **7 β** emission, indicating a FRET process from **9 α** as an energy donor to **7 β** as the energy acceptor, and is supported by overlapped emission spectra of the donor and absorbance spectra of the acceptor nucleoside (Fig. 14c and d). Therefore, while interaction between the donor–acceptor β -nucleosides (**9 β /7 β**) reveals non-FRET quenching of the acceptor β -butyropyrenyltriazole nucleoside (**7 β**), a FRET-based enhanced emission of the β -nucleoside (**7 β**) is observed while titrating with an acceptor α -nucleoside (**9 α**).

We next explored the novel triazolyl butyramidopyrene nucleoside **7 β** ($^{T\text{BPy}}B_{\text{Do}}$) for studying interactions with BSA protein. The UV-visible absorption of nucleoside **7 β** in phosphate buffer showed a structured absorption characteristic of

pyrene at around 313, 326 and 342 nm. Addition of an increasing concentration of BSA to the probe solution resulted in a structured absorption that experienced strong hyperchromicity along with a bathochromic shift of 2–4 nm of all the bands. The BSA absorption at 280 nm also shifted to 285 nm. The bathochromic shift indicated that pyrene was accommodated in the hydrophobic region, which was also supported by the absorption of the pyrene moiety in various organic solvents (Fig. 9). These observations indicated a ground state binding interaction between BSA and nucleoside **7β**, most probably in the hydrophobic region (Fig. 15a). We next carried out fluorescence titration experiments. In phosphate buffer the nucleoside **7β** showed strong emission bands at 376, 397 and 414 nm which correspond to pyrene-structured emissions. A comparison of the BSA emission and the absorption spectra of nucleoside **7β** revealed that there is a possibility of a FRET process that occurs from BSA to the **TBPy** moiety of nucleoside **7β** (ESI, Fig. S2†). Thus, when excited at the absorption maximum of BSA (280 nm) wherein there was very weak absorption of nucleoside **7β**, and comparing the emission spectrum of only BSA with that of only the nucleoside and a 1 : 1 mixture of BSA : nucleoside, it was observed that the emission intensity of the nucleoside **7β** increased while that of BSA decreased (Fig. 15b and ESI, Fig. S2†). This observation clearly suggests that the probe nucleoside is accommodated inside the hydrophobic pocket of BSA and the **TBPy** moiety of nucleoside **7β** faces closer to one of the tryptophans of BSA, leading to a FRET process from tryptophan to **TBPy**. Upon gradual addition of an increasing amount of BSA, the emission from the **TBPy** moiety also increased gradually. However, the change in inten-

sity is not so drastic, indicating a weak interaction between the probe nucleoside and BSA inside the hydrophobic pocket in an excited state. That the probe nucleoside **7β** (**^{TBPy}B_{Do}**) resided on the hydrophobic pocket and experienced highly restricted rotational motion was evident from an enhancement of the fluorescence anisotropy from 0.003 to 0.02 (ESI, Fig. S2†).³⁰ Finally, we thought that a mixture of the donor-acceptor nucleosides could interact with BSA differently. For that purpose a 1 : 1 mixture of the donor nucleoside **7β** and the acceptor nucleoside **9α** was considered as a probe, and the probe solution was titrated with an increasing concentration of BSA. The UV-visible spectra with pyrene absorption experience a drastic hyperchromicity along with a red-shift of 3–5 nm of the vibronic bands of pyrene at 326 and 342 nm as the concentration of BSA increases. Moreover, the buried absorption of the acceptor nucleoside also is found to increase as the BSA concentration increases (Fig. 15c). This observation indicates a strong interaction between BSA and the donor-acceptor mixture in the hydrophobic pocket of BSA. Upon excitation at the pyrene absorption at 342 nm and increasing the concentration of BSA led to a little or almost no quenching of the pyrene emission. However, on excitation at the BSA absorption of 280 nm, an overall quenching of the emission of the probe, both in the pyrene or in the triazolylcyanobenzene region, is observed (Fig. 15d). This might be because of FRET quenching in the hydrophobic pocket. That the probe resided in the hydrophobic pocket of BSA was evident from an increased anisotropy from 0.006 to 0.06.³⁰ Therefore, the fluorescence results show that the interaction of the 1 : 1 mixture of the **7β/9α** nucleosides with BSA is the opposite to the interaction between nucleoside **7β** only and BSA. All the results suggested that both hydrophobic as well as electrostatic interactions played an important role in the present interaction study between the probe nucleoside **7β** (**^{TBPy}B_{Do}**)/BSA and a 1 : 1 mixture **7β/9α** and BSA.

Conclusion

We have synthesized some new triazolyl nucleosides *via* an azide-alkyne cycloaddition reaction as a key step of the synthesis with very good yields, and their photophysical properties in various organic solvents have been evaluated. The alkynes are commercially available and cheap and the azides can easily be accessed from the chlorosugar. These nucleosides, particularly as donor-acceptor pairs in DNA, are expected to show interesting π - π stacking and photophysical properties. Biophysical studies in the DNA context with the unexplored bases are our current research target. We also exploited one of the triazolyl nucleosides in studying the interaction process with BSA and found that hydrophobic as well as electrostatic interactions played an important role in the sensing of BSA by the probe nucleoside **7β** (**^{TBPy}B_{Do}**). Also, under study are the noncovalent interactions of pyrenyl nucleosides, in particular, with proteins.

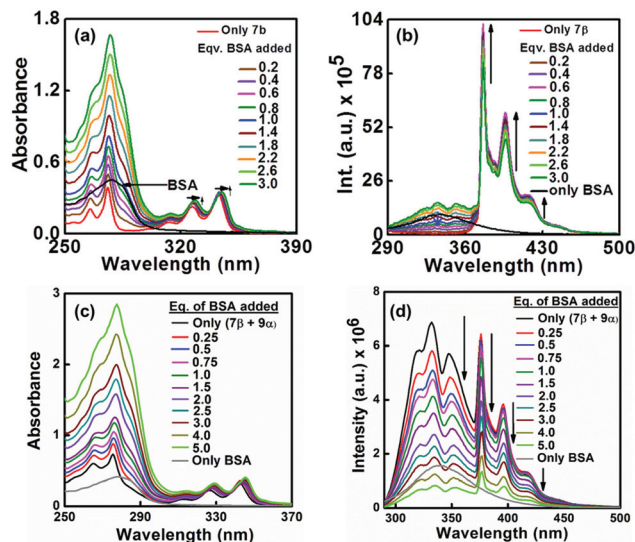


Fig. 15 (a) Absorption titration of the probe nucleoside **7β** (**^{TBPy}B_{Do}**) upon addition of a gradually increasing concentration of BSA. (b) Steady state emission of the probe nucleoside **7β** (**^{TBPy}B_{Do}**) in the absence or in the presence of BSA showing a FRET process and gradual enhancement of the probe emission. (c–d) Absorption and fluorescence titration of a 1 : 1 mixture of **7β/9α** [10 μ M] with an increasing concentration of BSA (at λ_{ex} = 280 nm; probe concentration is 10 μ M).

Experimental section

General experimental and materials

^1H NMR spectra were recorded on a 400 MHz machine; ^{13}C NMR spectra were measured at 100 MHz. The coupling constant (J value) is reported in hertz. The chemical shifts are shown in ppm downfield from tetramethylsilane, using residual chloroform ($\delta = 7.24$ in ^1H NMR, $\delta = 77.0$ in ^{13}C NMR), dimethyl sulfoxide ($\delta = 2.48$ in ^1H NMR, $\delta = 39.5$ in ^{13}C NMR) and/or methanol ($\delta = 3.30$ in ^1H NMR, $\delta = 49.0$ in ^{13}C NMR) as an internal standard. Melting point (mp) was recorded (in some cases) on a microscopic melting point apparatus. Fast atom bombardment (FAB) masses and/or HRMS were recorded on a high resolution mass spectrometer. BSA, Na_2HPO_4 and $\text{NaH}_2\text{PO}_4 \cdot \text{H}_2\text{O}$ (for preparation of the phosphate buffer) were purchased from Merck, India and used without further purification. Water was taken from a Milli-Q purification system. All solutions were prepared 1 hour before the experiments were done. The probe molecules [nucleoside $^{\text{TBPY}}\text{B}_{\text{Do}}$ (**7 β**)] were synthesized and purified according to the procedure described.

Synthesis of 2-deoxy-3,5-di-*O*-*p*-toluoyl- α -D-ribofuranosyl chloride (10**).**²⁰ The synthesis of bis-toluoyl-protected Hoffer's chlorosugar **10** was achieved starting from 2-deoxyribose sugar (4 g, 29.8 mmol) with an overall yield of 4.48 g (59%, 0.01 mol) following our published protocol.²⁰

Synthesis of 2-deoxy-3,5-bis[*O*-(*p*-toluoyl)]- β -D-ribofuranosyl-azide (11**, Method A).**³¹ The β -azido sugar was synthesised *via* the reaction of toluoyl-protected chloro-deoxyribose sugar (**10**, 1 eq., 1.5 g, 3.86 mmol) and cesium azide (CsN_3) (1.2 eq., 4.63 mmol, 0.81 g) in dry DMSO following our literature procedure with 90% yield (1.37 g).³¹

Synthesis of 2-deoxy-3,5-bis[*O*-(*p*-toluoyl)]- α -D-ribofuranosyl-azide (12**) (Method B).**^{20,22,23,31} The α -azido sugar (**12**) was synthesised following our earlier report utilising a $\text{BF}_3 \cdot \text{Et}_2\text{O}$ (0.1 eq., 0.386 mmol, 4.76 ml)-mediated reaction of toluoyl-protected chloro-deoxyribose sugar (**10**, 1.5 g, 3.86 mmol) and trimethylsilylazide (TMS-N_3) (1.2 eq., 4.63 mmol, 0.61 ml) at 0 °C in dry DCM to afford the α -azido sugar (**12**) in 59% (0.9 g) yield.^{20,22,23,31}

General procedure for the synthesis of the triazolyl donor/acceptor aromatic nucleosides *via* "Click" reaction

In a two necked round bottomed flask, α - and/or β -azido-deoxyribose sugar (1.0 equiv.) was taken and dry THF was added. The solution was then degassed by purging with N_2 gas for 10 min. While continuing degassing, the aromatic alkyne (1.5 equiv.) was added through the side neck followed by addition of 6 mol% of sodium ascorbate dissolved in a small quantity of water. After that 1 mol% of copper sulphate dissolved in a small quantity of water was added through the side neck. The reaction mixture was further degassed for another 5 min. The final ratio of THF: H_2O in the reaction mixture was maintained at 3:1. Finally, diisopropylethylamine (DIPEA) was added to the reaction mixture and was refluxed at 75–80 °C for about 12 hours. After completion of the reaction monitored by

TLC, the reaction mixture was evaporated and partitioned between water and ethyl acetate. The organic layer was washed with water twice, then with brine solution twice and finally kept over Na_2SO_4 for drying. Next the reaction mixture was filtered and concentrated by evaporation. The products were then separated by column chromatography and characterized. The average isolated yields were between 90–99%.

Synthesis of 3',5'-bis[*O*-(*p*-toluoyl)]-2'-deoxy-1'- β -triazolyl-*N,N*-dimethylaminobenzene nucleoside (13 β** , bis-toluoyl- β - $^{\text{TNDMB}}\text{B}_{\text{Do}}$).** Using the general procedure, starting from 60 mg of β -azido-deoxyribose sugar (**11**, 0.15 mmol) and 26.14 mg of 1-ethynyl-*N,N*-dimethylaniline (alkyne **A**, 0.18 mmol), 78.26 mg (0.145 mmol) of the triazolyl-*N,N*-dimethylaminobenzene nucleoside **13 β** was isolated as a yellow solid. Yield 96.6%; mp 185–188 °C; IR (KBr) 1721, 1612, 1508, 1296, 1279, 1109 cm^{-1} ; ^1H NMR (CDCl_3 , 400 MHz) δ 2.38 (3H, s), 2.44 (3H, s), 2.99 (6H, s), 3.12–3.18 (2H, m), 4.57 (1H, dd, $J = 3.6, 11.6$ Hz), 4.65–4.72 (2H, m), 5.77–5.79 (1H, m), 6.54 (1H, t, $J = 6.8$ Hz), 6.7 (2H, d, $J = 8.8$ Hz), 7.2 (2H, d, $J = 7.6$ Hz), 7.28 (2H, d, $J = 8.0$ Hz), 7.54 (2H, d, $J = 8.8$ Hz), 7.79 (1H, s), 7.89 (2H, d, $J = 8.0$ Hz), 7.96 (2H, d, $J = 8.4$ Hz); ^{13}C NMR (CDCl_3 , 100 MHz) δ 21.8, 38.6, 40.52, 64.0, 74.9, 83.6, 88.9, 112.5, 116.6, 118.6, 126.6, 126.8, 129.4, 129.8, 129.9, 144.2, 144.6, 148.8, 150.6, 166.0, 166.3; HRMS calcd for $\text{C}_{31}\text{H}_{33}\text{N}_4\text{O}_5$ [$\text{M} + \text{H}$]⁺ 541.2445, found 541.2485.

Synthesis of 3',5'-bis[*O*-(*p*-toluoyl)]-2'-deoxy-1'- α -triazolyl-*N,N*-dimethylaminobenzene nucleoside (13 α** , bis-toluoyl- α - $^{\text{TNDMB}}\text{B}_{\text{Do}}$).** Using the general procedure, starting from 50 mg of α -azido-deoxyribose sugar (**12**, 0.126 mmol) and 22.071 mg of 1-ethynyl-*N,N*-dimethylaniline (alkyne **A**, 0.607 mmol), 58.9 mg (0.109 mmol) of the triazolyl-*N,N*-dimethylaminobenzene nucleoside **13 α** was isolated as a yellow solid. Yield 86.5%; mp 158–160 °C; IR (KBr) 1718, 1611, 1377, 1309, 1102 cm^{-1} ; ^1H NMR (CDCl_3 , 400 MHz) δ 2.33 (3H, s), 2.4 (3H, s), 2.96 (6H, s), 2.99–3.14 (2H, m), 4.55–4.64 (2H, m), 4.8–4.84 (1H, m), 5.65 (1H, d, $J = 5.6$ Hz), 6.53 (1H, d, $J = 6.4$ Hz), 6.73 (2H, d, $J = 8.8$ Hz), 7.09 (2H, d, $J = 7.6$ Hz), 7.24 (2H, d, $J = 8$ Hz), 7.66 (2H, d, $J = 8$ Hz), 7.7 (2H, d, $J = 8$ Hz), 7.94 (2H, d, $J = 8.0$ Hz), 7.98 (1H, s); ^{13}C NMR (CDCl_3 , 100 MHz) δ 21.7, 38.7, 40.5, 64.1, 74.7, 84.8, 89.9, 112.5, 116.5, 118.9, 126.3, 126.8, 129.4, 129.8, 144.2, 144.3, 148.4, 150.5, 165.9, 166.2; HRMS calcd for $\text{C}_{31}\text{H}_{33}\text{N}_4\text{O}_5$ [$\text{M} + \text{H}$]⁺ 541.2445, found 541.2440.

Synthesis of 3',5'-bis[*O*-(*p*-toluoyl)]-2'-deoxy-1'- β -triazolyl-dimethoxyphenyl nucleoside (14 β** , bis-toluoyl- β - $^{\text{TDMB}}\text{B}_{\text{Do}}$).** This was synthesized and characterized according to our published protocol.²⁰

Synthesis of 3',5'-bis[*O*-(*p*-toluoyl)]-2'-deoxy-1'- α -triazolyl-dimethoxyphenyl nucleoside (14 α** , bis-toluoyl- α - $^{\text{TDMB}}\text{B}_{\text{Do}}$).** Using the general procedure, starting from 200 mg (**12**, 0.506 mmol) of α -azido-deoxyribose sugar and 98.45 mg (alkyne **B**, 0.607 mmol) of 1-ethynyl-3,5-dimethoxybenzene, 267.6 mg (0.480 mmol) of the triazolyl-dimethoxyphenyl nucleoside **14 α** was isolated as a colourless gel. Yield 95%; IR (KBr) 3145, 1720, 1611, 1269 cm^{-1} . ^1H NMR (CDCl_3 , 400 MHz) δ 2.21 (3H, s), 2.29 (3H, s), 2.9–3.01 (2H, m), 3.68 (6H, s), 4.45–4.52 (2H,

m), 4.71–4.74 (1H, m), 5.54–5.55 (1H, m), 6.33 (1H, t, $J = 2.4$ Hz), 6.45–6.47 (1H, m), 6.86 (2H, d, $J = 2.4$ Hz), 6.98 (2H, d, $J = 8$ Hz), 7.13 (2H, d, $J = 8$ Hz), 7.56 (2H, d, $J = 8$ Hz), 7.83 (2H, d, $J = 8$ Hz), 8.01 (1H, s); ^{13}C NMR (CDCl_3 , 100 MHz) δ 21.6, 21.7, 38.8, 55.4, 64.0, 74.7, 85.1, 90.2, 100.7, 103.7, 118.4, 126.2, 126.7, 129.3, 129.4, 129.6, 129.7, 132.3, 144.3, 144.5, 147.7, 161.2, 165.9, 166.2; HRMS calcd for $\text{C}_{31}\text{H}_{32}\text{N}_3\text{O}_7$ $[\text{M} + \text{H}]^+$ 558.2235, found 558.2232.

Synthesis of 3',5'-bis(O-(*p*-toluoyl))-2'-deoxy-1'- β -triazolylphenoxyphenyl nucleoside (15 β , bis-toluoyl- β - $^{\text{TPHOB}}\text{B}_{\text{Do}}$). Using the general procedure, starting from 60 mg (11, 0.152 mmol) of β -azido-deoxyribose sugar and 35.4 mg (alkyne C, 0.182 mmol) of 1-ethynyl-phenoxybenzene, 80.60 mg (0.137 mmol) of the triazolylphenoxyphenyl nucleoside 15 β was isolated as a white solid. Yield 90%; IR (KBr) 1721, 1612, 1508, 1296, 1279, 1109 cm^{-1} ; ^1H NMR (CDCl_3 , 400 MHz) δ 2.36 (3H, s), 2.44 (3H, s), 2.89–2.93 (1H, m), 3.13–3.19 (1H, m), 4.56 (1H, dd, $J = 4, 12$ Hz), 4.68–4.78 (2H, m), 5.79–5.80 (1H, m), 6.56 (1H, t, $J = 6.2$ Hz), 6.99 (2H, d, $J = 8.4$ Hz), 7.04 (2H, d, $J = 8.4$ Hz), 7.13–7.15 (1H, m), 7.19 (2H, d, $J = 8$ Hz), 7.26–7.29 (3H, m), 7.34–7.38 (2H, m), 7.59 (2H, d, $J = 8.8$ Hz), 7.86–7.88 (2H, m), 7.96 (2H, d, $J = 8$ Hz); ^{13}C NMR (CDCl_3 , 100 MHz) δ 21.81, 38.8, 63.9, 74.9, 83.8, 89.2, 117.7, 119.1, 119.2, 123.7, 125.5, 126.6, 126.8, 127.4, 129.1, 129.5, 129.8, 129.9, 144.4, 144.7, 147.9, 157.1, 157.5, 166.1, 166.3; HRMS calcd for $\text{C}_{35}\text{H}_{32}\text{N}_3\text{O}_6$ $[\text{M} + \text{H}]^+$ 590.2286, found 590.2287.

Synthesis of 3',5'-bis(O-(*p*-toluoyl))-2'-deoxy-1'- α -triazolylphenoxyphenyl nucleoside (15 α , bis-toluoyl- α - $^{\text{TPHOB}}\text{B}_{\text{Do}}$). Using the general procedure, starting from 50 mg (12, 0.126 mmol) of α -azido-deoxyribose sugar and 29.3 mg (alkyne C, 0.152 mmol) of ethynylphenoxybenzene, 38.5 mg (0.065 mmol) of the triazolylphenoxyphenyl nucleoside 15 α was isolated as a white solid. Yield 51.85%; mp 129–130 $^\circ\text{C}$; IR (KBr) 1718, 1699, 1278, 1244, 1178, 1109 cm^{-1} ; ^1H NMR (CDCl_3 , 400 MHz) δ 2.26 (3H, s), 2.35 (3H, s), 2.93–3.10 (2H, m), 4.49–4.59 (2H, m), 4.74–4.77 (1H, m), 5.59 (1H, d, $J = 6.4$ Hz), 6.49 (1H, d, $J = 6$ Hz), 6.95–7.07 (7H, m), 7.19 (2H, d, $J = 8$ Hz), 7.28 (2H, t, $J = 8$ Hz), 7.59 (2H, d, $J = 8$ Hz), 7.68 (2H, d, $J = 8.8$ Hz), 7.87 (2H, d, $J = 8.4$ Hz), 7.99 (1H, s); ^{13}C NMR (CDCl_3 , 100 MHz) δ 21.9, 38.9, 64.1, 74.8, 74.8, 85.2, 90.3, 117.7, 119.2, 123.7, 125.9, 126.4, 126.9, 127.5, 129.4, 129.5, 129.8, 129.9, 130.0, 144.5, 144.6, 147.6, 157.2, 157.6, 166.1, 166.3; HRMS calcd for $\text{C}_{34}\text{H}_{32}\text{N}_3\text{O}_6$ $[\text{M} + \text{H}]^+$ 590.2286, found 590.2283.

Synthesis of 3',5'-bis(O-(*p*-toluoyl))-2'-deoxy-1'- β -triazolylmethoxynaphthalene nucleoside (16 β , bis-toluoyl- β - $^{\text{TMNap}}\text{B}_{\text{Do}}$).³¹ This was synthesized and characterized according to our published protocol.³¹ Thus, using the general procedure, starting from 60 mg (0.152 mmol) of β -azidodeoxyribose sugar (11) and 33.16 mg (alkyne D, 0.182 mmol) of 2-ethynyl-6-methoxynaphthalene, 87.04 mg (0.151 mmol) of the triazolylmethoxynaphthalene nucleoside 16 β was isolated as a brown solid. Yield 99.3%; mp 197–200 $^\circ\text{C}$; $R_f = 0.45$ in 2 : 1 (v/v) hexane–ethyl acetate; HRMS calcd for $\text{C}_{34}\text{H}_{32}\text{N}_3\text{O}_6$ $[\text{M} + \text{H}]^+$ 578.2286, found 578.2365.²⁹

Synthesis of 3',5'-bis(O-(*p*-toluoyl))-2'-deoxy-1'- α -triazolylmethoxynaphthalene nucleoside (16 α , bis-toluoyl- α - $^{\text{TMNap}}\text{B}_{\text{Do}}$).

Using the general procedure, starting from 50 mg (12, 0.126 mmol) of α -azido-deoxyribose sugar and 27.52 mg (alkyne D, 0.151 mmol) of 2-ethynyl-6-methoxynaphthalene, 71.3 mg (0.123 mmol) of the triazolylmethoxynaphthalene nucleoside 16 α was isolated as a white solid. Yield 98%; mp 144–148 $^\circ\text{C}$; IR (KBr) 3154, 1717, 1611, 1270, 851, 819, 750, 690 cm^{-1} ; ^1H NMR (CDCl_3 , 400 MHz) δ 2.27 (3H, s), 2.41 (3H, s), 3.03–3.16 (2H, m), 3.94 (3H, s), 4.59–4.68 (2H, m), 4.87–4.88 (1H, m), 5.69 (1H, d, $J = 6.4$ Hz), 6.62 (1H, d, $J = 6.8$ Hz), 7.05 (2H, d, $J = 8$ Hz), 7.13–7.17 (2H, m), 7.26 (2H, d, $J = 8$ Hz), 7.68–7.71 (3H, m), 7.75 (1H, d, $J = 8.4$ Hz), 7.86–7.88 (1H, m), 7.96 (2H, d, $J = 8$ Hz), 8.17 (1H, s), 8.19 (1H, s); ^{13}C NMR (CDCl_3 , 100 MHz) δ 21.7, 21.8, 38.9, 55.4, 64.1, 74.9, 85.1, 90.3, 105.9, 117.9, 119.4, 124.5, 125.9, 126.3, 126.8, 127.4, 129.1, 129.5, 129.7, 129.8, 134.5, 144.4, 144.6, 148.2, 158.1, 165.9, 166.3; HRMS calcd for $\text{C}_{34}\text{H}_{32}\text{N}_3\text{O}_6$ $[\text{M} + \text{H}]^+$ 578.2286, found 578.2296.

Synthesis of 3',5'-bis(O-(*p*-toluoyl))-2'-deoxy-1'- β -triazolylphenanthrene nucleoside (17 β , bis-toluoyl- β - $^{\text{TPhen}}\text{B}_{\text{Do}}$). This was synthesized and characterized according to our published protocol.²⁰

Synthesis of 3',5'-bis(O-(*p*-toluoyl))-2'-deoxy-1'- α -triazolylphenanthrene nucleoside (17 α , bis-toluoyl- α - $^{\text{TPhen}}\text{B}_{\text{Do}}$). Using the general procedure, starting from 200 mg (0.506 mmol) of α -azido-deoxyribose sugar (12) and 122.77 mg (alkyne E, 0.607 mmol) of 9-ethynylphenanthrene, 288.7 mg (0.483 mmol) of the triazolylphenanthrene nucleoside 17 α was isolated as a yellow gel. Yield 95.5%; IR (KBr) 1719, 1611, 1270, 1100, 752, 728 cm^{-1} ; ^1H NMR (CDCl_3 , 400 MHz) δ 2.24 (3H, s), 2.44 (3H, s), 3.07–3.14 (1H, m), 3.29–3.3 (1H, m), 4.61–4.71 (2H, m), 4.9–4.91 (1H, m), 5.70 (1H, d, $J = 6.8$ Hz), 6.69 (1H, d, $J = 6$ Hz), 7.00 (2H, d, $J = 8$ Hz), 7.29 (2H, d, $J = 7.6$ Hz), 7.51–7.55 (1H, m), 7.59–7.71 (5H, m), 7.81 (1H, d, $J = 7.6$ Hz), 7.88 (1H, s), 7.97 (2H, d, $J = 8$ Hz), 8.22 (1H, s), 8.38 (1H, d, $J = 8$ Hz), 8.71 (1H, d, $J = 8$ Hz), 8.77 (1H, d, $J = 8$ Hz); ^{13}C NMR (CDCl_3 , 100 MHz) δ 21.6, 21.7, 39.1, 64.1, 74.8, 85.2, 90.4, 121.2, 122.6, 122.9, 126.2, 126.4, 126.8, 126.9, 126.9, 127.2, 128.5, 128.8, 129.4, 129.7, 129.8, 130.1, 130.5, 130.7, 131.3, 144.3, 144.4, 146.9, 165.9, 166.2; HRMS calcd for $\text{C}_{37}\text{H}_{32}\text{N}_3\text{O}_5$ $[\text{M} + \text{H}]^+$ 598.2336, found 598.2333.

Synthesis of 3',5'-bis(O-(*p*-toluoyl))-2'-deoxy-1'- α -triazolylpyrene nucleoside (18 β , bis-toluoyl- β - $^{\text{TPy}}\text{B}_{\text{Do}}$). Using the general procedure, starting from 100 mg (11, 0.253 mmol) of β -azido-deoxyribose sugar and 68.59 mg (alkyne F, 0.304 mmol) of 1-ethynylpyrene, 133.63 mg (0.215 mmol) of the triazolylpyrene nucleoside 18 β was isolated as a yellow solid. Yield 85%; IR (KBr) 2926, 1719, 1610, 1278 cm^{-1} ; ^1H NMR (CDCl_3 , 400 MHz) δ 2.16 (3H, s), 2.45 (3H, s), 2.98–3.04 (1H, m), 3.29–3.36 (1H, m), 4.63 (1H, dd, $J = 3.2, 11.2$ Hz), 4.74–4.79 (2H, m), 5.86–5.87 (1H, m), 6.69 (1H, t, $J = 6.4$ Hz), 7.03 (1H, d, $J = 8$ Hz), 7.29 (2H, d, $J = 7.6$ Hz), 7.89 (2H, d, $J = 8$ Hz), 7.98–8.11 (8H, m), 8.16–8.22 (4H, m), 8.63 (1H, d, $J = 8$ Hz); ^{13}C NMR (CDCl_3 , 100 MHz) δ 21.9, 38.9, 64.0, 74.9, 83.9, 89.3, 121.6, 124.9, 125.3, 125.6, 126.3, 126.6, 127.3, 127.5, 128.1, 128.4, 128.8, 129.4, 129.5, 129.8, 130.0, 144.3, 144.7, 148.1, 166.1, 166.4; HRMS calcd for $\text{C}_{39}\text{H}_{33}\text{N}_3\text{O}_5$ $[\text{M} + 2\text{H}]^+$ 623.2420, found 623.2454.

Synthesis of 3',5'-bis(*O*-(*p*-toluoyl))-2'-deoxy-1'- α -triazolylbutylpyrene nucleoside (19 β , bis-toluoyl- β -^{TBP}B_{Do}). Using the general procedure, starting from 50 mg (11, 0.126 mmol) of β -azido-deoxyribose sugar and 47.06 mg (alkyne G, 0.151 mmol) of pyrenebutyric acid *N*-propynyl amide, 86.00 mg (0.122 mmol) of the triazolylbutylpyrene nucleoside 19 β was isolated as a dirty white solid. Yield 94.58%; IR (KBr) 3334.6, 2942.2, 1726.1, 1650.5, 1610, 1278 cm⁻¹; ¹H NMR (CDCl₃, 400 MHz) δ 2.16–2.22 (2H, m), 2.27 (1H, d, *J* = 8 Hz), 2.33 (3H, s), 2.42 (3H, s), 2.76–2.82 (1H, m), 3.17–3.24 (1H, m), 3.35 (1H, t, *J* = 8 Hz), 4.43–4.63 (5H, m), 4.53–4.55 (1H, m), 5.71–5.74 (1H, m), 6.14–6.16 (1H, m), 6.38 (1H, t, *J* = 6 Hz), 7.15 (2H, d, *J* = 8 Hz), 7.25 (2H, d, *J* = 8 Hz), 7.69 (1H, s), 7.79–7.83 (3H, m), 7.91–8.00 (6H, m), 8.08 (2H, d, *J* = 8 Hz), 8.13–8.16 (2H, m), 8.26 (1H, d, *J* = 8.8 Hz); ¹³C NMR (CDCl₃, 100 MHz) δ 20.0, 20.2, 27.9, 31.3, 33.1, 33.8, 35.8, 62.7, 73.3, 81.3, 86.6, 120.8, 122.2, 123.3, 124.6, 125.1, 125.3, 125.8, 126.1, 127.1, 127.7, 127.8, 128.1, 128.2, 129.3, 129.7, 135.1, 142.3, 142.7, 144.2, 164.1, 164.2, 171.1; HRMS calcd for C₄₄H₄₂N₄O₆ [M + 2H]⁺ 722.3104, found 722.3107.

Synthesis of 3',5'-bis(*O*-(*p*-toluoyl))-2'-deoxy-1'- β -triazolylnitrophenyl nucleoside (20 β , bis-toluoyl- β -^{TNB}B_{Ac}). This was synthesized and characterized according to our published protocol.²⁰

Synthesis of 3',5'-bis(*O*-(*p*-toluoyl))-2'-deoxy-1'- α -triazolylnitrophenyl nucleoside (20 α , bis-toluoyl- α -^{TNB}B_{Ac}). Using the general procedure, starting from 200 mg (0.506 mmol) of azido-deoxyribose sugar (12) and 89.31 mg (0.607 mmol) of 1-ethynyl-4-nitrobenzene, 268.8 mg (0.496 mmol) of compound 20 α was isolated as a yellow solid. Yield 98%; mp 180–182 °C; IR (KBr) 1716, 1610, 1514, 1339 cm⁻¹; ¹H NMR (CDCl₃, 400 MHz) δ 2.34 (3H, s), 2.43 (3H, s), 3.04–3.23 (2H, m), 4.59–4.69 (2H, m), 4.86–4.89 (1H, m), 5.68 (1H, d, *J* = 6 Hz), 6.6 (1H, d, *J* = 5.6 Hz), 7.07 (2H, d, *J* = 8 Hz), 7.28 (2H, d, *J* = 8 Hz), 7.63 (2H, d, *J* = 8.0 Hz), 7.95 (4H, d, *J* = 8.4 Hz), 8.24 (1H, s), 8.26 (1H, s), 8.27 (1H, s); ¹³C NMR (CDCl₃, 100 MHz) δ 21.9, 38.9, 64.0, 74.8, 85.4, 90.5, 119.7, 124.4, 126.3, 126.8, 129.4, 129.5, 129.7, 129.9, 136.9, 144.5, 144.8, 145.8, 147.5, 165.9, 166.3; HRMS calcd for C₂₉H₂₇N₄O₇ [M + H]⁺ 543.1874, found 543.1879.

Synthesis of 3',5'-bis(*O*-(*p*-toluoyl))-2'-deoxy-1'- β -triazolylcyanophenyl nucleoside (21 β , bis-toluoyl- β -^{TCNB}B_{Ac}). This was synthesized and characterized according to our published protocol.²⁰

Synthesis of 3',5'-bis(*O*-(*p*-toluoyl))-2'-deoxy-1'- α -triazolylcyanophenyl nucleoside (21 α , bis-toluoyl- α -^{TCNB}B_{Ac}). Using the general procedure, starting from 200 mg (0.506 mmol) of α -azido-deoxyribose sugar (12) and 77.199 mg (0.607 mmol) of 4-ethynylbenzotrile, 250.65 mg (0.480 mmol) of compound 21 α was isolated as a white solid. Yield 95%; mp 160–163 °C; IR (KBr) 2226, 1717, 1611, 1104 cm⁻¹; ¹H NMR (CDCl₃, 400 MHz) δ 2.35 (3H, s), 2.43 (3H, s), 3.03–3.1 (1H, m), 3.17–3.2 (1H, m), 4.58–4.68 (2H, m), 4.84–4.86 (1H, m), 5.67 (1H, d, *J* = 8 Hz), 6.59 (1H, d, *J* = 6.8 Hz), 7.06 (2H, d, *J* = 8 Hz), 7.28 (2H, d, *J* = 8.4 Hz), 7.62 (2H, d, *J* = 8 Hz), 7.69 (2H, d, *J* = 8.8 Hz), 7.9 (2H, d, *J* = 8.6 Hz), 7.95 (2H, d, *J* = 8 Hz), 8.21 (1H,

s); ¹³C NMR (CDCl₃, 100 MHz) δ 21.9, 39.0, 64.0, 74.8, 85.4, 90.5, 118.9, 119.4, 126.2, 129.4, 129.5, 129.7, 129.9, 132.9, 144.5, 144.8, 146.1, 165.9, 166.3; HRMS calcd for C₃₀H₂₇N₄O₅ [M + H]⁺ 523.1976, found 523.1974.

Synthesis of 3',5'-bis(*O*-(*p*-toluoyl))-2'-deoxy-1'- β -triazolylformylbenzene nucleoside (22 β , bis-toluoyl- β -^{TBenzal}B_{Ac}). Using the general procedure, starting from 60 mg (0.152 mmol) of β -azido-deoxyribose sugar (11) and 23.69 mg (0.182 mmol) of 4-ethynylbenzaldehyde, 77.75 mg (0.148 mmol) of compound 22 β was isolated as a white solid. Yield 97.4%; mp 188–190 °C; IR (KBr) 2852, 1727, 1714, 1695, 1610, 1280, 1112 cm⁻¹; ¹H NMR (CDCl₃, 400 MHz) δ 2.36 (3H, s), 2.45 (3H, s), 2.94–2.96 (1H, m), 3.16–3.19 (1H, m), 4.54–4.57 (1H, m), 4.70 (1H, s), 4.76–4.79 (1H, m), 5.80–5.82 (1H, d, *J* = 2.4 Hz), 6.58 (1H, t, *J* = 6 Hz), 7.18 (1H, d, *J* = 7.2 Hz), 7.29 (2H, d, *J* = 8 Hz), 7.79 (2H, d, *J* = 7.6 Hz), 7.84–7.88 (4H, m), 7.96 (2H, d, *J* = 8 Hz), 8.05 (1H, s), 10.02 (1H, s); ¹³C NMR (DMSO-*d*₆, 100 MHz) δ 21.9, 38.0, 64.8, 75.5, 83.7, 89.4, 122.9, 126.7, 127.6, 127.7, 130.2, 130.2, 130.4, 130.6, 131.1, 136.8, 137.2, 144.8, 145.2, 146.9, 166.4, 166.5, 193.1; HRMS calcd for C₃₀H₂₈N₃O₆ [M + 2H]⁺ 526.1973, found 526.1982.

Synthesis of 3',5'-bis(*O*-(*p*-toluoyl))-2'-deoxy-1'- α -triazolylformylbenzene nucleoside (22 α , bis-toluoyl- α -^{TBenzal}B_{Ac}). Using the general procedure, starting from 50 mg (0.126 mmol) of α -azido-deoxyribose sugar (12) and 19.65 mg (0.151 mmol) of 4-ethynylbenzaldehyde, 52 mg (0.099 mmol) of compound 22 α was isolated as a white solid. Yield 78.5%; mp 142–145 °C; IR (KBr) 1717, 1694, 1610, 1286, 1107 cm⁻¹; ¹H NMR (CDCl₃, 400 MHz) δ 2.23 (3H, s), 2.33 (3H, s), 2.94–3.11 (2H, m), 4.49–4.58 (2H, m), 4.78 (1H, s), 5.59 (1H, d, *J* = 5.6 Hz), 6.51 (1H, d, *J* = 6.8 Hz), 6.96 (2H, d, *J* = 7.6 Hz), 7.17 (2H, d, *J* = 8 Hz), 7.54 (2H, d, *J* = 7.6 Hz), 7.8–7.88 (6H, m), 8.16 (1H, s), 9.92 (1H, s); ¹³C NMR (CDCl₃, 100 MHz) δ 21.7, 21.8, 38.9, 64.0, 74.8, 85.3, 90.4, 119.7, 126.1, 126.2, 126.8, 129.4, 129.5, 129.7, 129.8, 130.4, 135.9, 136.4, 144.4, 144.7, 146.6, 165.9, 166.2, 191.8; HRMS calcd for C₃₀H₂₈N₃O₆ [M + H]⁺ 526.1973, found 526.1973.

Synthesis of 3',5'-bis(*O*-(*p*-toluoyl))-2'-deoxy-1'- β -triazolyl difluorophenyl nucleoside (23 β , bis-toluoyl- β -^{TDFB}B_{Ac}). Using the general procedure, starting from 60 mg (0.152 mmol) of β -azido-deoxyribose sugar (11) and 25 mg (0.182 mmol) of 1-ethynyl-2,4-difluorobenzene, 69.6 mg (0.130 mmol) of compound 23 β was isolated as a white solid. Yield 86%; mp 165–170 °C; IR (KBr) 1729, 1709, 1610, 1281, 1112 cm⁻¹; ¹H NMR (CDCl₃, 400 MHz) δ 2.36 (3H, s), 2.44 (3H, s), 2.88–2.92 (1H, m), 3.26–3.29 (1H, m), 4.56 (1H, dd, *J* = 4, 12 Hz), 4.65–4.69 (2H, m), 5.8–5.81 (1H, m), 6.54 (1H, t, *J* = 6 Hz), 6.82–6.88 (1H, m), 6.98 (1H, t, *J* = 8 Hz), 7.16 (2H, d, *J* = 8 Hz), 7.28 (2H, d, *J* = 8 Hz), 7.84 (2H, d, *J* = 8 Hz), 7.96 (2H, d, *J* = 8 Hz), 8.08–8.09 (1H, m), 8.18–8.25 (1H, m); ¹³C NMR (CDCl₃, 100 MHz) δ 21.8, 21.9, 38.4, 63.9, 74.9, 83.8, 89.1, 104.2, 111.9, 112.1, 121.3, 126.6, 126.8, 129.3, 129.4, 129.8, 129.95, 141.1, 144.1, 144.6, 166.01, 166.29; HRMS calcd for C₂₉H₂₆F₂N₃O₅ [M + H]⁺ 534.1835, found 534.1886.

Synthesis of 3',5'-bis(*O*-(*p*-toluoyl))-2'-deoxy-1'- α -triazolyl difluorophenyl nucleoside (23 α , bis-toluoyl- α -^{TDFB}B_{Ac}). Using the

general procedure, starting from 50 mg (0.126 mmol) of α -azido-deoxyribose sugar (**12**) and 20.88 mg (0.151 mmol) of 1-ethynyl-2,4-difluorobenzene, 66.65 mg (0.125 mmol) of compound **23 α** was isolated as a white solid. Yield 99.2%; mp 117–120 °C; IR (KBr) 1716, 1610, 1281, 1270, 1101 cm^{-1} ; ^1H NMR (CDCl_3 , 400 MHz) δ 2.24 (3H, s), 2.32 (3H, s), 2.96–3.02 (1H, m), 3.06 (1H, d, $J = 14.8$ Hz), 4.49–4.58 (2H, m), 4.74–4.77 (1H, m), 5.59 (1H, d, $J = 6.4$ Hz), 6.51 (1H, d, $J = 5.2$ Hz), 6.75–6.81 (1H, m), 6.88–6.93 (1H, m), 6.99 (2H, d, $J = 8$ Hz), 7.17 (2H, d, $J = 8$ Hz), 7.58 (2H, d, $J = 8$ Hz), 7.86 (2H, d, $J = 8$ Hz), 8.14 (1H, d, $J = 3.6$ Hz), 8.15–8.21 (1H, m); ^{13}C NMR (CDCl_3 , 100 MHz) δ 21.8, 38.9, 64.1, 74.7, 85.1, 90.3, 103.9, 104.2, 104.4, 111.9, 112.2, 120.6, 120.7, 126.2, 126.8, 129.0, 129.1, 129.3, 129.5, 129.8, 140.8, 144.4, 144.5, 166.1, 166.3; HRMS calcd for $\text{C}_{29}\text{H}_{26}\text{F}_2\text{N}_3\text{O}_5$ $[\text{M} + \text{H}]^+$ 534.1835, found 534.1837.

General procedure for toluoyl deprotection of the triazolyl donor/acceptor aromatic nucleosides

The bis-toluoylated nucleoside (1 equiv.) was dissolved in dry methanol. Sodium methoxide (3.5 equiv.) was subsequently added. The solution was left stirring at room temperature overnight. The solution was evaporated and the deprotected products were separated by column chromatography. All the β -epimers except **22 β** ($^{\text{TBenzal}}\text{B}_{\text{Ac}}$) and **23 β** ($^{\text{TDFB}}\text{B}_{\text{Ac}}$) were deprotected. None of the α -epimers were deprotected.

Synthesis of 2'-deoxy-1'- β -triazolyl-*N,N*-dimethylanilino nucleoside (1 β** , β - $^{\text{TNDMB}}\text{B}_{\text{Do}}$).** Using the general procedure for deprotection starting from 98.2 mg (0.182 mmol) of compound **13 β** , 50.4 mg (0.165 mmol) of compound **1 β** was isolated as a yellow solid. Yield 91.11%; mp 168 °C; IR (KBr) 3330, 1617, 1507, 1201, 1105, 1051, 1013 cm^{-1} ; ^1H NMR (CD_3OD , 400 MHz) δ 2.36–2.42 (1H, m), 2.64–2.71 (1H, m), 2.84 (6H, s), 3.49–3.54 (1H, m), 3.59–3.64 (1H, m), 3.90 (1H, q, $J = 4.2, 4.8$ Hz), 4.43 (1H, q, $J = 4.6, 6$ Hz), 6.29 (1H, t, $J = 6$ Hz), 6.68 (2H, d, $J = 8.4$ Hz), 7.51 (2H, d, $J = 8.8$ Hz), 8.21 (1H, s); ^{13}C NMR (CD_3OD , 100 MHz) δ 40.9, 41.9, 63.5, 72.5, 89.9, 90.4, 113.9, 119.3, 119.8, 127.8, 149.8, 152.4; HRMS calcd for $\text{C}_{15}\text{H}_{21}\text{N}_4\text{O}_3$ $[\text{M} + \text{H}]^+$ 305.1608, found 305.1643.

Synthesis of 2'-deoxy-1'- β -triazolyl-dimethoxyphenyl nucleoside (2 β** , $^{\text{TDMB}}\text{B}_{\text{Do}}$).** This was synthesized and characterized according to our published protocol.²⁰

Synthesis of 2'-deoxy-1'- α -triazolyl-dimethoxyphenyl nucleoside (2 α** , α - $^{\text{TDMB}}\text{B}_{\text{Do}}$).** Using the general procedure for deprotection starting from 260 mg (0.47 mmol) of compound **14 α** , 144.0 mg (0.448 mmol) of compound **2 α** was isolated as a white solid. Yield 95.4%; IR (KBr) 3340, 1208, 1082, 1053 cm^{-1} ; ^1H NMR (CD_3OD , 400 MHz) δ 2.40 (1H, td, $J = 2.4, 14.4$ Hz), 2.73–2.80 (1H, m), 3.49–3.53 (1H, m), 3.56–3.60 (1H, m), 3.70 (6H, s), 4.16 (1H, q, $J = 3.6$ Hz), 4.32–4.35 (1H, m), 6.33 (1H, d, $J = 2.4$ Hz), 6.35 (1H, d, $J = 2.0$ Hz), 6.87 (2H, d, $J = 2.4$ Hz), 8.47 (1H, s); ^{13}C NMR (CD_3OD , 100 MHz) δ 42.0, 56.0, 63.3, 72.7, 90.7, 91.5, 101.6, 104.8, 121.22, 130.3, 130.9, 133.5, 148.9, 162.9; HRMS calcd for $\text{C}_{15}\text{H}_{20}\text{O}_5\text{N}_3$ $[\text{M} + \text{H}]^+$ 322.1402, found 322.1416.

Synthesis of 2'-deoxy-1'- β -triazolyl-phenoxyphenyl nucleoside (3 β** , β - $^{\text{TPhOB}}\text{B}_{\text{Do}}$).** Using the general procedure for deprotection starting from 100.00 mg (0.169 mmol) of compound **15 β** , 54.1 mg (0.153 mmol) of compound **3 β** was isolated as a white solid. Yield 90.67%; mp 143 °C; IR (KBr) 3399, 1488, 1241, 1090, 1067, 1039 cm^{-1} ; ^1H NMR (CD_3OD , 400 MHz) δ 2.52–2.55 (1H, m), 2.79–2.83 (1H, m), 3.64–3.77 (2H, m), 4.04–4.07 (1H, m), 4.56–4.59 (1H, m), 6.43–6.45 (1H, m), 7.01 (4H, d, $J = 6.8$ Hz), 7.13 (1H, t, $J = 6.0$ Hz.), 7.36 (2H, t, $J = 6.4$ Hz), 7.78 (2H, d, $J = 7.2$ Hz), 8.45 (1H, s); ^{13}C NMR (CD_3OD , 100 MHz) δ 41.9, 63.4, 72.4, 89.9, 90.5, 120.1, 120.4, 120.6, 124.9, 126.8, 128.5, 131.2, 148.7, 158.4, 159.2; HRMS calcd for $\text{C}_{19}\text{H}_{20}\text{O}_4\text{N}_3$ $[\text{M} + \text{H}]^+$ 354.1453, found 354.1480.

Synthesis of 2'-deoxy-1'- β -triazolylmethoxynaphthalene nucleoside (4 β** , β - $^{\text{MNAp}}\text{B}_{\text{Do}}$).**³¹ This was synthesized in a similar way as we reported previously.³¹ Thus, using the general procedure for deprotection starting from 85 mg (0.147 mmol) of compound **16 β** , 52.92 mg (0.153 mmol) of compound **4 β** was isolated as a white solid. Yield 88%; $R_f = 0.5$ in 100% ethyl acetate; mp 141–145 °C; HRMS calcd for $\text{C}_{18}\text{H}_{20}\text{N}_3\text{O}_4$ $[\text{M} + \text{H}]^+$ 342.1453, found 342.1479.²⁹

Synthesis of 2'-deoxy-1'- α -triazolylmethoxynaphthalene nucleoside (4 α** , α - $^{\text{MNAp}}\text{B}_{\text{Do}}$).** Using the general procedure for deprotection starting from 280 mg (0.48 mmol) of compound **16 α** , 141.1 mg (0.413 mmol) of compound **4 α** was isolated as a white solid. Yield 86%; mp 183–185 °C; IR (KBr) 3353, 1611, 1502, 1261, 1218, 1142, 1106, 861, 815 cm^{-1} ; ^1H NMR (CD_3OD , 400 MHz) δ 2.42 (1H, td, $J = 2.4, 14.4$ Hz), 2.75–2.82 (1H, m), 3.51–3.61 (2H, m), 3.79 (3H, s), 4.18 (1H, q, $J = 3.6, 4.0$ Hz), 4.34–4.37 (1H, m), 6.37 (1H, dd, $J = 2.4, 7.6$ Hz), 7.03 (1H, dd, $J = 2.4, 9.2$ Hz), 7.13 (1H, d, $J = 2.4$ Hz), 7.67–7.77 (3H, m), 8.10 (1H, s), 8.56 (1H, s); ^{13}C NMR (DMSO, 100 MHz) δ 55.3, 61.4, 70.4, 88.5, 88.9, 106.0, 119.2, 119.5, 123.5, 124.1, 125.9, 127.4, 128.6, 129.6, 133.9, 146.7, 157.5; HRMS calcd for $\text{C}_{18}\text{H}_{20}\text{O}_4\text{N}_3$ $[\text{M} + \text{H}]^+$ 342.1453, found 342.1466.

Synthesis of 2'-deoxy-1'- β -triazolylphenanthrene nucleoside (5 β** , β - $^{\text{TPhen}}\text{B}_{\text{Do}}$).** This was synthesized and characterized according to our published protocol.²⁰

Synthesis of 2'-deoxy-1'- α -triazolylphenanthrene nucleoside (5 α** , α - $^{\text{TPhen}}\text{B}_{\text{Do}}$).** Using the general procedure for deprotection starting from 280 mg (0.486 mmol) of compound **17 α** , 145.9 mg (0.404 mmol) of compound **5 α** was isolated as a pale yellow solid. Yield 83%; IR (KBr) 3364, 1121 1056, 857, 841, 746, 728 cm^{-1} ; ^1H NMR (CD_3OD , 400 MHz) δ 2.50 (1H, td, $J = 2.4, 14.4$ Hz), 2.79–2.87 (1H, m), 3.52–3.63 (2H, m), 4.23 (1H, q, $J = 3.8, 3.2$ Hz), 4.36–4.39 (1H, m), 6.47 (1H, dd, $J = 2, 7.4$ Hz), 7.48–7.53 (2H, m), 7.56–7.61 (2H, m), 7.83 (1H, d, $J = 8.0$ Hz), 7.85 (1H, s), 8.11 (1H, d, $J = 8.4$ Hz), 8.52 (1H, s), 8.66 (1H, d, $J = 8.4$ Hz), 8.73 (1H, d, $J = 8.0$ Hz); ^{13}C NMR (CD_3OD , 100 MHz) δ 42.4, 63.6, 73.0, 91.2, 92.0, 124.1, 124.4, 124.6, 127.4, 128.4, 128.5, 128.9, 129.9, 130.3, 131.7, 132.1, 132.4, 132.9, 148.0; HRMS calcd for $\text{C}_{21}\text{H}_{20}\text{N}_3\text{O}_3$ $[\text{M} + \text{H}]^+$ 362.1499, found 362.1498.

Synthesis of 2'-deoxy-1'- β -triazolylpyrene nucleoside (6 β** , β - $^{\text{TPy}}\text{B}_{\text{Do}}$).**³² Using the general procedure for deprotection starting from 60 mg (0.097 mmol) of compound **18 β** , 30.61 mg

(0.080 mmol) of compound **6β** was isolated as a white solid. Yield 81.4%; IR (KBr) 3376.8, 2942.5, 1068 cm⁻¹; ¹H NMR (CD₃OD + CDCl₃, 400 MHz) δ 2.64–2.68 (1H, m), 2.95–2.99 (1H, m), 3.73–3.86 (2H, m), 4.13 (1H, s), 4.55 (1H, s), 6.60 (1H, t, *J* = 5.6 Hz), 8.03–8.29 (8H, m), 8.56 (1H, d, *J* = 8 Hz), 8.67 (1H, s); ¹³C NMR (CD₃OD, 100 MHz) δ 38.88, 41.39, 62.65, 71.59, 89.41, 89.79, 123.69, 125.56, 125.79, 126.04, 126.38, 127.23, 128.13, 128.68, 128.92, 129.06, 131.65, 132.19, 147.69; HRMS calcd for C₂₃H₂₁N₃O₃ [M + 2H]⁺ 387.1583, found 387.1532.

Synthesis of 2'-deoxy-1'-β-triazolybutylpyrene nucleoside (7β, β-TBP^{Py}B_{Do}). Using the general procedure for deprotection starting from 50 mg (0.069 mmol) of compound **19β**, 27.88 mg (0.058 mmol) of compound **7β** was isolated as a white solid. Yield 83%; IR (KBr) 3432, 3356.8, 2926.8, 1715 cm⁻¹; ¹H NMR (CD₃OD, 400 MHz) δ 1.99–2.07 (2H, m), 2.25 (2H, t, *J* = 7.2 Hz), 2.29–2.35 (1H, m), 2.55–2.61 (1H, m), 3.19–3.24 (2H, m) (merged with solvent peak), 3.24–3.58 (2H, m), 3.89 (1H, q, *J* = 4.4 Hz), 4.27–4.39 (3H, m), 6.24 (1H, t, *J* = 6 Hz), 7.74 (1H, d, *J* = 7.6 Hz), 7.84–8.06 (8H, m), 8.16 (1H, d, *J* = 9.2 Hz); ¹³C NMR (CD₃OD, 100 MHz) δ 30.9, 33.8, 35.8, 36.7, 41.9, 63.4, 72.4, 89.8, 90.3, 123.1, 124.5, 125.9, 126.0, 126.2, 126.3, 127.1, 127.8, 128.4, 128.5, 128.6, 129.9, 131.4, 132.4, 132.9, 137.4, 146.6, 175.93; HRMS calcd for C₂₈H₃₀N₄O₄ [M + 2H]⁺ 486.2267, found 486.2230.

Synthesis of 2'-deoxy-1'-β-triazolynitrophenyl nucleoside (8β, β-TNB^{B_{Ac}}). This was synthesized and characterized according to our published protocol.²⁰

Synthesis of 2'-deoxy-1'-α-triazolynitrophenyl nucleoside (8α, α-TNB^{B_{Ac}}). Using the general procedure for deprotection starting from 290 mg (0.54 mmol) of compound **20α**, 135.5 mg (0.442 mmol) of compound **8α** was isolated as a yellow solid. Yield 82%; mp 147–150 °C; IR (KBr) 3523, 3473, 1513, 1341, 857 cm⁻¹; ¹H NMR (CD₃OD, 400 MHz) δ 2.52–2.57 (1H, m), 2.87–2.94 (1H, m), 3.63–3.74 (2H, m), 4.30–4.33 (1H, m), 4.46–4.49 (1H, m), 6.5–6.5 (1H, dd, *J* = 2, 7.6 Hz), 8.07 (2H, d, *J* = 8.8 Hz), 8.3 (2H, d, *J* = 8.8 Hz), 8.8 (1H, s); ¹³C NMR (CD₃OD, 100 MHz) δ 42.2, 63.4, 72.7, 91.0, 91.8, 122.7, 125.5, 127.5, 138.4, 146.9, 148.9; ESI calcd for C₁₃H₁₅N₄O₅ [M + H]⁺ 307.1042, found 307.1376.

Synthesis of 2'-deoxy-1'-β-triazolycyanophenyl nucleoside (9β, β-TCNB^{B_{Ac}}). This was synthesized and characterized according to our published protocol.²⁰

Synthesis of 2'-deoxy-1'-α-triazolycyanophenyl nucleoside (9α, α-TCNB^{B_{Ac}}). Using the general procedure for deprotection starting from 240 mg (0.46 mmol) of compound **21α**, 123.5 mg (0.431 mmol) of compound **9α** was isolated as a white solid. Yield 93.8%; mp 124–129 °C; IR (KBr) 3450, 3403, 2232, 1085 cm⁻¹; ¹H NMR (CD₃OD, 400 MHz) δ 2.40 (1H, td, *J* = 2, 14.8 Hz), 2.73–2.80 (1H, m), 3.49–3.54 (1H, m), 3.56–3.59 (1H, m), 4.17 (1H, q, *J* = 3.8, 7.0 Hz), 4.32–4.35 (1H, m), 6.37 (1H, dd, *J* = 2, 7.6 Hz), 7.67 (2H, d, *J* = 8.4 Hz), 7.89 (2H, d, *J* = 8.4 Hz), 8.64 (1H, s); ¹³C NMR (CD₃OD, 100 MHz) δ 42.1, 63.3, 72.9, 90.9, 91.8, 112.6, 122.4, 127.2, 127.4, 136.5, 147.1; HRMS calcd for C₁₄H₁₅N₄O₃ [M + H]⁺ 287.1144, found 287.1147.

Crystallographic description and ORTEP diagram

Crystal data were collected with a CCD diffractometer using graphite monochromated MoKα radiation ($\lambda = 0.71073 \text{ \AA}$) at 298 K. Cell parameters were retrieved using and refined with softwares on all observed reflections.³³ Data reduction was performed with the software and corrected for Lorentz and polarization effects.³³ Absorption corrections were applied with the program.³⁴ The structure was solved by direct methods implemented in a program and refined by full-matrix least-squares methods on F^2 .³⁵ All non-hydrogen atomic positions were located in difference Fourier maps and refined anisotropically. The hydrogen atoms were placed in their geometrically generated positions. Colourless crystals were isolated, of rectangular shape, from acetonitrile at room temperature.

Crystallographic description for 2'-deoxy-1'-β-triazolynitrobenzene nucleoside (8β, β-TNB^{B_{Ac}}). Crystal dimension (mm): 0.30 × 0.26 × 0.17. C₁₃H₁₄N₄O₅, Mr = 306.28; orthorhombic, space group *P*212121; *a* = 6.4456(7) Å, *b* = 9.8102(8) Å, *c* = 21.8210(19) Å; $\alpha = 90.00^\circ$, $\beta = 90.00^\circ$, $\gamma = 90.00^\circ$, *V* = 1379.8(2) Å³; *Z* = 4; $\rho_{\text{cal}} = 1.474 \text{ g cm}^{-3}$; $\mu \text{ (mm}^{-1}\text{)} = 0.116$; *F*(000) = 640.00; refinement method = full-matrix least-squares on F^2 ; final *R* indices [*I* > 2 σ] *R*(reflections) = 0.0509(1701), *wR*₂(reflections) = 0.1143(3180); goodness of fit = 0.933.

Crystallographic description for 2'-deoxy-1'-α-triazolynitromethoxyphenyl nucleoside (4α, α-MNAP^{B_{Do}}). Crystal dimension (mm): 0.29 × 0.22 × 0.15. C₁₈H₁₉N₃O₄, Mr = 341.36; monoclinic, space group *P*21; *a* = 5.808(7) Å, *b* = 29.856(4) Å, *c* = 9.539(11) Å; $\alpha = 90.00^\circ$, $\beta = 90.185^\circ$, $\gamma = 90.00^\circ$, *V* = 1654.2(4) Å³; *Z* = 4; $\rho_{\text{cal}} = 1.371 \text{ g cm}^{-3}$; $\mu \text{ (mm}^{-1}\text{)} = 0.099$; *F*(000) = 720.00; refinement method = full-matrix least-squares on F^2 ; final *R* indices [*I* > 2 σ] *R*(reflections) = 0.0478(2923), *wR*₂(reflections) = 0.1066(4410); goodness of fit = 0.989.

Photophysical studies of the nucleosides

UV-visible measurements. All the UV-visible spectra of the compounds (10 μM) were measured in different solvents using a UV-visible spectrophotometer with a cell of 1 cm path length. The measurements were carried out in the absorbance mode. The absorbance values of the sample solutions were measured in the wavelength regime of 200–550 nm. All the sample solutions were prepared just before doing the experiment.

Fluorescence experiments. All the sample solutions were prepared as described in the UV measurement experiments. Fluorescence spectra were obtained using a fluorescence spectrophotometer at 25 °C using a 1 cm path length cell. The excitation wavelengths for all the cases were set at the excitation maxima of each sample in each solvent, and emission spectra were measured in the wavelength regime of 300–700 nm with an integration time of 0.2 s. All the sample solutions were prepared just before doing the experiment. A total volume of 1.0 ml from a stock solution of 2 ml of 10 μM concentration for each case was used for the fluorescence experiments in a 1 ml cell. Fluorescence emissions were collected by exciting the samples at the wavelength corresponding

to their absorption maximum. Steady-state fluorescence emission spectra were recorded at room temperature as an average of five scans using an excitation slit of 3.0 nm, emission slit of 3.0 nm, and a scan speed of 120 nm min⁻¹. The fluorescence quantum yields (Φ_f) were determined using quinine sulphate as a reference with the known Φ_f (0.55) in 0.1 molar solution in sulphuric acid. The following equation was used to calculate the quantum yield:

$$\Phi_S = \Phi_R \frac{F_S^{\text{Area}} \text{Abs}_R n_S^2}{F_R^{\text{Area}} \text{Abs}_S n_R^2}$$

where Φ_R is the quantum yield of a standard reference, F_S^{Area} (sample) and F_R^{Area} (reference) are the integrated emission peak areas, Abs_S (sample) and Abs_R (reference) are the absorbances at the excitation wavelength, and n_S (sample) and n_R (reference) are the refractive indices of the solutions.

The fluorescence lifetime experiments were carried out using a time resolved fluorescence spectrophotometer at 25 °C using a 1 cm path length cell. A 375 nm laser was used as the excitation light source. The lifetime data were calculated by software with a fixed fitting range. The time correlated single photon counting (TCSPC) method was used to calculate the lifetime data. The lifetime data (Global Analysis) were calculated by the software package with a fitting range of 205–4000 channels.

Studies on the interaction of nucleoside ^{TBPy}B_{Do} (7β) with BSA

Preparation of BSA solution. Phosphate buffer of pH 7.0 was used to prepare the solution of BSA (Merck). A 250 μM of stock BSA solution was prepared by dissolving 0.0222 g of BSA in 1.28 mL phosphate buffer (20 mM) of pH 7.0. From that stock solution a sub-stock of 1000 μM BSA was prepared. The compound stock solution was prepared in DMF because of the poor solubility in water. 0.6 mg of nucleoside ^{TBPy}B_{Do} (7β) or 1 : 1 mixture of 7β : 9α as the probe was dissolved in 1 mL DMF to make a stock probe solution of concentration 1092.4 μM.

General experimental on interaction studies of BSA by photophysical studies. All the spectral measurements were carried out at room temperature. To study the interaction of compounds with BSA, an aqueous solution of the nucleoside ^{TBPy}B_{Do} (7β) or 1 : 1 mixture of 7β : 9α as the probe (10 μM for nucleoside) was titrated with different concentrations of BSA (ranging from 0, 0.2, 0.4, 0.6, 0.8, 1.0, 1.4, 1.8, 2.2, 2.6, 3.0 equivalents). The total volume of the final solution for each sample was 3 mL. The % of DMF content was 2%. The presence of 2% DMF does not induce structural changes to biomolecules. Each sample solution was mixed well before spectral measurements.

UV-visible study with BSA. The UV-visible absorbance measurements were performed using a Shimadzu UV-2550 UV-visible spectrophotometer with a cell of 1 cm path length at 298 K. All the UV-visible studies were carried out in 20 mM phosphate buffer of pH 7.02 containing solution at 298 K. 2% DMF was used to solubilize the probe. The measurements were taken in the absorbance mode and the absorbance values

of the sample solutions were measured in the wavelength regime of 200–700 nm. All the experiments were carried out with freshly prepared sample solutions.

Fluorescence study with BSA. All fluorescence and steady state anisotropy experiments were performed using a Fluoromax 4 spectrophotometer with a cell of 1 cm path length at 298 K. The excitation wavelength for the probe (nucleoside ^{TBPy}B_{Do} (7β) or 1 : 1 mixture of 7β : 9α as the probe) was set at 280 nm and 350 nm, and emission spectra were measured in the wavelength regime of 290–650 nm. Steady state anisotropy of the solutions was measured using Fluoromax 4 spectrophotometer.

Acknowledgements

This work is financially supported by the Department of Science and Technology [DST: SR/SI/OC-69/2008] and the Department of Biotechnology [DBT: BT/PR5169/BRB/10/1065/2012], Govt. of India.

Notes and references

- 1 A. Rich, M. Kasha and B. Pullmann, *Horizons in Biochem.*, 1962, p. 103.
- 2 (a) C. Switzer, S. E. Moroney and S. A. Benner, *J. Am. Chem. Soc.*, 1989, **111**, 8322; (b) C. Y. Switzer, S. E. Moroney and S. A. Benner, *Biochemistry*, 1993, **32**, 10489; (c) D. Hutter and S. A. Benner, *J. Org. Chem.*, 2003, **68**, 9839; (d) U. V. Krosigk and S. A. Benner, *Helv. Chim. Acta*, 2004, **87**, 1299; (e) Z. Yang, D. Hutter, P. Sheng, A. M. Sismour and S. A. Benner, *Nucleic Acids Res.*, 2006, **34**, 6095; (f) T. A. Martinot and S. A. Benner, *J. Org. Chem.*, 2004, **69**, 3972; (g) J. J. Vogell, U. von Krosigk and S. A. Benner, *J. Org. Chem.*, 1993, **58**, 7542; (h) S. A. Benner, *Acc. Chem. Res.*, 2004, **37**, 784; (i) J. J. Voegel and S. A. Benner, *J. Am. Chem. Soc.*, 1994, **116**, 6929.
- 3 (a) Y. Tor and P. B. Devran, *J. Am. Chem. Soc.*, 1993, **115**, 4461; (b) I. Hirao, M. Kimoto, T. Mitsui, T. Fujiwara, R. Kawai, A. Sato, Y. Harada and S. Yokoyama, *Nat. Methods*, 2006, **3**, 729; (c) Y. Doi, J. Chiba, T. Morikawa and M. Inouye, *J. Am. Chem. Soc.*, 2008, **130**, 8762; (d) J. C. Delaney, J. Gao, H. Liu, N. Shrivastav, J. M. Essigmann and E. T. Kool, *Angew. Chem., Int. Ed.*, 2009, **48**, 4524.
- 4 (a) H. Echols and M. F. Goodman, *Annu. Rev. Biochem.*, 1991, **60**, 477; (b) P. Strazewski and C. Tamm, *Angew. Chem., Int. Ed. Engl.*, 1990, **29**, 36; (c) Y. J. Seo, S. Matsuda and F. E. Romesberg, *J. Am. Chem. Soc.*, 2009, **131**, 5046; (d) Y. N. Teo, J. N. Wilson and E. T. Kool, *J. Am. Chem. Soc.*, 2009, **131**, 3923.
- 5 (a) A. Okamoto, Y. Saito and I. Saito, *J. Photochem. Photobiol., C*, 2005, **6**, 108; (b) S. S. Bag, R. Kundu, K. Matsumoto, Y. Saito and I. Saito, *Bioorg. Med. Chem.*

- Letts.*, 2010, **20**, 3227; (c) Y. N. Teo and E. T. Kool, *Chem. Rev.*, 2012, **112**, 4221.
- 6 (a) B. A. Schweitzer and E. T. Kool, *J. Am. Chem. Soc.*, 1995, **117**, 1863; (b) E. T. Kool, *Annu. Rev. Biochem.*, 2002, **71**, 191; (c) Y. J. Seo, S. Matsuda and F. E. Romesberg, *J. Am. Chem. Soc.*, 2009, **131**, 5046; (d) S. K. Jarchow-Choy, E. Sjuvarsson, H. O. Sintim, S. Eriksson and E. T. Kool, *J. Am. Chem. Soc.*, 2009, **131**, 5488.
- 7 (a) A. A. Henry and F. E. Romesberg, *Curr. Opin. Chem. Biol.*, 2003, **7**, 727; (b) E. T. Kool, *Acc. Chem. Res.*, 2002, **35**, 936; (c) E. T. Kool, J. C. Morales and K. M. Guckian, *Angew. Chem., Int. Ed.*, 2000, **39**, 990.
- 8 (a) A. M. Sismour and S. A. Benner, *Nucleic Acids Res.*, 2005, **33**, 5640; (b) A. M. Leconte, L. Chen and F. E. Romesberg, *J. Am. Chem. Soc.*, 2005, **127**, 12470; (c) I. Hirao, M. Kimoto, T. Mitsui, T. Fujiwara, R. Kawai, A. Sato, Y. Harada and S. Yokoyama, *Nat. Methods*, 2006, **3**, 729.
- 9 (a) H.-J. Kim, N. A. Leal, S. Hoshika and S. A. Benner, *J. Org. Chem.*, 2014, **79**, 3194; (b) O. Khakshoor, S. E. Wheeler, K. N. Houk and E. T. Kool, *J. Am. Chem. Soc.*, 2012, **134**, 3154; (c) S. A. Benner, *Acc. Chem. Res.*, 2004, **37**, 784; (d) C. R. Geyer, T. R. Battersby and S. A. Benner, *Structure*, 2003, **11**, 1485; (e) Z. Yang, D. Hutter, P. Sheng, A. M. Sismour and S. A. Benner, *Nucleic Acids Res.*, 2006, **34**, 6095; (f) K. C. Schneider and S. A. Benner, *J. Am. Chem. Soc.*, 1990, **112**, 453; (g) H. Lu, A. T. Krueger, J. Gao, H. Liu and E. T. Kool, *Org. Biomol. Chem.*, 2010, **8**, 2704; (h) H. O. Sintim and E. T. Kool, *J. Am. Chem. Soc.*, 2009, **131**, 11270; (i) J. C. Delaney, J. Gao, H. Liu, N. Shrivastav, J. M. Essigmann and E. T. Kool, *Angew. Chem., Int. Ed.*, 2009, **48**, 4524; (j) N. Minakawa, S. Ogata, M. Takahashi and A. Matsuda, *J. Am. Chem. Soc.*, 2009, **131**, 1644; (k) I. Hirao, M. Kimoto, S.-I. Yamakage, M. Ishikawa, J. Kikuchi and S. Yokoyama, *Bioorg. Med. Chem. Lett.*, 2002, **12**, 1391; (l) K. Gao, *Recent Res. Dev. Nucleosides Nucleotides*, 2003, **1**, 97; (m) Y. Kim, A. M. Leconte, Y. Hari and F. E. Romesberg, *Angew. Chem., Int. Ed.*, 2006, **45**, 7809; (n) I. Hirao, *CSJ Curr. Rev.*, 2011, **6**, 101; (o) R. Tawarada, K. Seio and M. Sekine, *J. Org. Chem.*, 2008, **73**, 383; (p) F.-A. Polonius and J. Mueller, *Angew. Chem., Int. Ed.*, 2007, **46**, 5602; (q) H. Liu, J. Gao, S. R. Lynch, Y. D. Saito, L. Maynard and E. T. Kool, *Science*, 2003, **302**, 868.
- 10 (a) B. A. Schweitzer and E. T. Kool, *J. Org. Chem.*, 1994, **59**, 7238; (b) B. A. Schweitzer and E. T. Kool, *J. Am. Chem. Soc.*, 1995, **117**, 1863; (c) R. X.-F. Ren, N. C. Chaudhuri, P. L. Paris, S. Rumney IV and E. T. Kool, *J. Am. Chem. Soc.*, 1996, **118**, 7671; (d) S. Moran, R. X.-F. Ren, S. Rumney IV and E. T. Kool, *J. Am. Chem. Soc.*, 1997, **119**, 2056; (e) S. Moran, R. X.-F. Ren and E. T. Kool, *Proc. Natl. Acad. Sci. U. S. A.*, 1997, **94**, 10506; (f) T. J. Matray and E. T. Kool, *J. Am. Chem. Soc.*, 1998, **120**, 6191; (g) J. C. Morales and E. T. Kool, *J. Am. Chem. Soc.*, 1999, **121**, 2323; (h) D. Barsky, E. T. Kool and M. E. Colvin, *J. Biomol. Struct. Dyn.*, 1999, **16**, 1119; (i) K. M. Guckian, T. R. Krugh and E. T. Kool, *J. Am. Chem. Soc.*, 2000, **122**, 6841; (j) E. T. Kool, *Acc. Chem. Res.*, 2002, **35**, 936; (k) Y. Takezawa and M. Shionoya, *Acc. Chem. Res.*, 2012, **45**, 2066; (l) T. Otsuka and T. Miyazaki, *Int. J. Quantum Chem.*, 2013, **113**, 504; (m) G. T. Hwang, Y. Hari and F. E. Romesberg, *Nucleic Acids Res.*, 2009, **37**, 4757; (n) I. Hirao, *Curr. Opin. Chem. Biol.*, 2006, **10**, 622; (o) I. Hirao, M. Kimoto, T. Mitsui, T. Fujiwara, R. Kawai, A. Sato, Y. Harada and S. Yokoyama, *Nat. Methods*, 2006, **3**, 729; (p) A. A. Henry and F. E. Romesberg, *Curr. Opin. Chem. Biol.*, 2003, **7**, 727; (q) K. Betz, D. A. Malyshev, T. Lavergne, W. Welte, K. Diederichs, F. E. Romesberg and A. Marx, *J. Am. Chem. Soc.*, 2013, **135**, 18637; (r) L. Li, M. Degardin, T. Lavergne, D. A. Malyshev, K. Dhimi, P. Ordoukhanian and F. E. Romesberg, *J. Am. Chem. Soc.*, 2014, **136**, 826; (s) T. Lavergne, M. Degardin, D. A. Malyshev, H. T. Quach, K. Dhimi, P. Ordoukhanian and F. E. Romesberg, *J. Am. Chem. Soc.*, 2013, **135**, 5408; (t) M. Kimoto and I. Hirao, *Methods Mol. Biol.*, 2010, **634**, 355.
- 11 (a) S. S. Bag, J. M. Heemstra, Y. Saito and D. M. Chenoweth, *J. Nucleic Acids*, 2012, 718582; (b) L. Li, M. Degardin, T. Lavergne, D. A. Malyshev, K. Dhimi, P. Ordoukhanian and F. E. Romesberg, *J. Am. Chem. Soc.*, 2014, **136**, 826–829; (c) M. Kimoto, Y. Hikida and I. Hirao, *Isr. J. Chem.*, 2013, **53**, 450–468; (d) I. Hirao and M. Kimoto, *Proc. Jpn. Acad., Ser. B*, 2012, **88**, 345–367; (e) D. A. Malyshev, K. Dhimi, H. T. Quach, T. Lavergne, P. Ordoukhanian, A. Torkamani and F. E. Romesberg, *Proc. Natl. Acad. Sci. U. S. A.*, 2012, **109**, 12005–12010; (f) R. Yamashige, M. Kimoto, Y. Takezawa, A. Sato, T. Mitsui, S. Yokoyama and I. Hirao, *Nucleic Acids Res.*, 2012, **40**, 2793–2806; (g) T. Lavergne, D. A. Malyshev and F. E. Romesberg, *Chem. – Eur. J.*, 2012, **18**, 1231–1239; (h) M. Kimoto, R. S. Cox III and I. Hirao, *Expert Rev. Mol. Diagn.*, 2011, **11**, 321–331; (i) A. T. Krueger, L. W. Peterson, J. Chelliserry, D. J. Kleinbaum and E. T. Kool, *J. Am. Chem. Soc.*, 2011, **133**, 18447–18451; (j) I. Hirao, M. Ed. Kimoto and G. Mayer, in *Chemical Biology of Nucleic Acids*, 2010, pp. 39–62; (k) M. Kimoto and I. Hirao, *Methods Mol. Biol.*, 2010, **634**, 355–369; (l) F. E. Romesberg, C. Yu, S. Matsuda and A. A. Henry, in *Current protocols in nucleic acid chemistry*, ed. L. B. Serge, 2002, ch. 1, unit 1.5.
- 12 (a) F. Wojciechowski and C. J. Leumann, *Chem. Soc. Rev.*, 2011, **40**, 5669; (b) N. A. Grigorenko and C. J. Leumann, *Chem. – Eur. J.*, 2009, **15**, 639; (c) J. N. Wilson, Y. N. Teo and E. T. Kool, *J. Am. Chem. Soc.*, 2007, **129**, 15426; (d) N. Robertson and C. A. McGowan, *Chem. Soc. Rev.*, 2003, **32**, 96; (e) K. Keren, M. Krueger, R. Gilad, G. Ben-Yoseph, U. Sivan and E. Braun, *Science*, 2002, **297**, 72; (f) D. B. Hall, R. E. Holmlin and J. K. Barton, *Nature*, 1996, **382**, 731.
- 13 (a) J. Liu, Z. Cao and Y. Lu, *Chem. Rev.*, 2009, **109**, 1948; (b) T. G. Drummond, M. G. Hill and J. K. Barton, *Nat. Biotechnol.*, 2003, **21**, 1192; (c) D. M. Kolpashchikov, Y. V. Gerasimova and M. S. Khan, *ChemBioChem*, 2011, **12**, 2564; (d) L. Liu, Y. Li, D. Liotta and S. Lutz, *Nucleic Acids Res.*, 2009, **37**, 4472.
- 14 (a) J. Stambasky, M. Hocek and P. Kouovsky, *Chem. Rev.*, 2009, **109**, 6729 and references therein. (b) E. T. Kool, *Acc.*

- Chem. Res.*, 2002, **35**, 936; (c) Y. Tor and P. B. Dervan, *J. Am. Chem. Soc.*, 1993, **115**, 4461; (d) G. H. Clever, C. Kaul and T. Carell, *Angew. Chem., Int. Ed.*, 2007, **46**, 6226.
- 15 (a) Li Han and Y. Bu, *Phys. Chem. Chem. Phys.*, 2011, **13**, 5906–5914; (b) Y. N. Teo and E. T. Kool, *Chem. Rev.*, 2012, **112**, 4221–4245; (c) M. Kimoto, T. Mitsui, R. Yamashige, A. Sato, S. Yokoyama and I. Hirao, *J. Am. Chem. Soc.*, 2010, **132**, 15418–15426; (d) M. Kimoto, T. Mitsui, S. Yokoyama and I. Hirao, *J. Am. Chem. Soc.*, 2010, **132**, 4988–4989; (e) J. Guo, S. Wang, N. Dai, Y. N. Teo and E. T. Kool, *Proc. Natl. Acad. Sci. U. S. A.*, 2011, **108**, 3493–3498; (f) N. Dai and E. T. Kool, *Chem. Soc. Rev.*, 2011, **40**, 5756–5770; (g) C.-K. Koo, S. Wang, R. L. Gaur, F. Samain, N. Banaei and E. T. Kool, *Chem. Commun.*, 2011, **47**, 11435–11437; (h) C.-K. Koo, F. Samain, N. Dai and E. T. Kool, *Chem. Sci.*, 2011, **2**, 1910–1917.
- 16 (a) F. Wojciechowski and C. J. Leumann, *Chem. Soc. Rev.*, 2011, **40**, 5669; (b) N. A. Grigorenko and C. J. Leumann, *Chem. – Eur. J.*, 2009, **15**, 639; (c) J. N. Wilson, Y. N. Teo and E. T. Kool, *J. Am. Chem. Soc.*, 2007, **129**, 15426; (d) N. Robertson and C. A. McGowan, *Chem. Soc. Rev.*, 2003, **32**, 96; (e) K. Keren, M. Krueger, R. Gilad, G. Ben-Yoseph, U. Sivan and E. Braun, *Science*, 2002, **297**, 72; (f) D. B. Hall, R. E. Holmlin and J. K. Barton, *Nature*, 1996, **382**, 731.
- 17 (a) J. Liu, Z. Cao and Y. Lu, *Chem. Rev.*, 2009, **109**, 1948; (b) T. G. Drummond, M. G. Hill and J. K. Barton, *Nat. Biotechnol.*, 2003, **21**, 1192; (c) D. M. Kolpashchikov, Y. V. Gerasimova and M. S. Khan, *ChemBioChem*, 2011, **12**, 2564; (d) L. Liu, Y. Li, D. Liotta and S. Lutz, *Nucleic Acids Res.*, 2009, **37**, 4472.
- 18 B. A. Ikkanda, S. A. Samuel and B. L. Iverson, *J. Org. Chem.*, 2014, **79**, 2029.
- 19 S. S. Bag and R. Kundu, *J. Org. Chem.*, 2011, **76**, 3348.
- 20 S. S. Bag, S. Talukdar, K. Matsumoto and R. Kundu, *J. Org. Chem.*, 2013, **78**, 278.
- 21 S. S. Bag, S. Talukdar and R. Kundu, *RSC Adv.*, 2013, **3**, 21352–21355.
- 22 (a) D.-W. Chen, A. E. Beuscher IV, R. C. Stevens, P. Wirsching, R. A. Lerner and K. D. Janda, *J. Org. Chem.*, 2001, **66**, 1725; (b) K. Yamada, H. Hayakawa, S. Sakata, N. Ashida and Y. Yoshimura, *Bioorg. Med. Chem. Lett.*, 2010, **20**, 6013–6016; (c) G. Deglane, F. Morvan, F. Debart and J.-J. Vasseur, *Bioorg. Med. Chem. Lett.*, 2007, **17**, 951–954; (d) T. Michel, F. Debart, F. Heitz and J.-J. Vasseur, *ChemBioChem*, 2005, **6**, 1254–1262; (e) F. Morvan, F. Debart and J.-J. Vasseur, *Chem. Biodiversity*, 2010, **7**, 494–535; (f) M. Sekine, Y. Seio, Y. Sato and K. Tateno, *Jpn. Kokai Tokkyo Koho*, JP2001253898A20010918, 2001; (g) H. Abdel Aleem, E. Larsen and E. B. Pedersen, *Tetrahedron*, 1995, **51**, 7867–7876.
- 23 (a) I. Štimac, I. Leban and J. Kobe, *Synlett*, 1999, 1069; (b) A. Štimac and J. Kobe, *Carbohydr. Res.*, 2000, **329**, 317; (c) R. Guezguez, K. Bougrin, K. E. Akri and R. Benhida, *Tetrahedron Lett.*, 2006, **47**, 4807; (d) P. Chittepup, V. R. Sirivolu and F. Seela, *Bioorg. Med. Chem.*, 2008, **16**, 8427; (e) V. Malnuit, M. Duca, A. Manout, K. Bougrin and R. Benhida, *Synlett*, 2009, 2123; (f) N. A. Kolganova, V. L. Florentiev, A. V. Chudinov, A. S. Zasedatelev and E. N. Timofeev, *Chem. Biodiversity*, 2011, **8**, 568.
- 24 (a) N. J. Turro, *Modern Molecular Photochemistry*, University Science Books, Sausalito, 1991; (b) J. R. Lakowicz, *Principles of Fluorescence Spectroscopy*, Springer, New York, 3rd edn, 2006; (c) S.-W. Yang, A. Elangovan, K.-C. Hwang and T.-I. Ho, *J. Phys. Chem. B*, 2005, **109**, 16628; (d) A. C. Benniston, A. Harriman, D. J. Lawrie and A. Mayeux, *Phys. Chem. Chem. Phys.*, 2004, **6**, 51; (e) A. C. Benniston, A. Harriman, D. J. Lawrie, A. Mayeux, K. Rafferty and O. D. Russell, *Dalton Trans.*, 2003, 4762; (f) J. G. Calvert and J. N. Pitts Jr., *Photochemistry*, John Wiley and Sons, Inc., New York, 1966; (g) S. A. Kovalenko, N. P. Ernsting and J. Ruthmann, *J. Chem. Phys.*, 1997, **106**, 3504; (h) B. Strehmel, H. Seifert and W. Rettig, *J. Phys. Chem. B*, 1997, **101**, 2232; (i) J. Kim and M. Lee, *J. Phys. Chem. A*, 1999, **103**, 3378; (j) P. Fromherz, *J. Phys. Chem.*, 1995, **99**, 7188.
- 25 (a) B. Albinsson, *J. Am. Chem. Soc.*, 1997, **119**, 6369; (b) X. Chen, Y. Zhao and Z. Cao, *J. Chem. Phys.*, 2009, **130**, 144307; (c) J. W. Verhoeven, T. Scherer and R. J. Willemse, *Pure Appl. Chem.*, 1993, **65**, 1717; (d) V. Thiagarajan, C. Selvaraju, E. J. P. Malar and P. Ramamurthy, *Chem-PhysChem*, 2004, **5**, 1200; (e) T. H. N. Pham and R. J. Clarke, *J. Phys. Chem. B*, 2008, **112**, 6513; (f) Y. Huang, T. Cheng, F. Li, C. Huang, T. Hou, A. Yu, X. Zhao and X. Xu, *J. Phys. Chem. B*, 2002, **106**, 10020; (g) A. S. R. Koti, B. Bhattacharjee, N. S. Haram, R. Das, N. Periasamy, N. D. Sonawane and D. W. Ragnekar, *J. Photochem. Photobiol., A*, 2000, **137**, 115; (h) T. Shim, M. H. Lee, D. Kim and Y. Ouchi, *J. Phys. Chem. B*, 2008, **112**, 1906; (i) D. Bingemann and N. P. Ernsting, *J. Chem. Phys.*, 1995, **102**, 2691; (j) N. Sertova, J.-M. Nunzi, I. Petkov and T. Deligeorgiev, *J. Photochem. Photobiol., A*, 1998, **112**, 187; (k) M. Panigrahi, S. Dash, S. Patel, P. K. Behera and B. K. Mishra, *Spectrochim. Acta, Part A*, 2007, **68**, 757.
- 26 (a) Z. R. Grabowski, K. Rotkiewicz and W. Rettig, *Chem. Rev.*, 2003, **103**, 3899; (b) G. M. Badger and I. S. Walker, *J. Chem. Soc.*, 1956, 122.
- 27 M. J. Frisch, *et al.*, *Gaussian 03 (revision C.02)*, Gaussian, Inc., Wallingford, CT, 2004.
- 28 (a) W. W. Parson, *Modern Optical Spectroscopy: With Examples from Biophysics and Biochemistry*, Springer-Verlag, Berlin Heidelberg, 2007; (b) G.-J. Zhao, J.-Y. Liu, L.-C. Zhou and K.-L. Han, *J. Phys. Chem. B*, 2007, **111**, 8940.
- 29 (a) S. S. Bag, S. Talukdar, R. Kundu, I. Saito and S. Jana, *Chem. Commun.*, 2014, **50**, 829–832; (b) T. Förster, *Naturwissenschaften*, 1946, **33**, 166; (c) M. R. Eftink, Fluorescence quenching: theory and applications, in *Topics in Fluorescence Spectroscopy*, ed. J. R. Lakowicz, Plenum Press, New York, NY, 1991, vol. 2, pp. 53–126; (d) B. Valeur and M. Berberan-Santos, *Molecular Fluorescence: Principles and Applications*, Wiley-VCH, Weinheim, 2nd edn, 2012; (e) Y. Ohiro, H. Ueda, N. Shibata and T. Nagamune, *Anal.*

- Biochem.*, 2007, **360**, 266; (f) T. Kato, H. Kashida, H. Kishida, H. Yada, H. Okamoto and H. Asanuma, *J. Am. Chem. Soc.*, 2013, **135**, 741; (g) Y. Saito, S. S. Bag, Y. Kusakabe, C. Nagai, K. Matsumoto, E. Mizuno, S. Kodate, I. Suzuka and I. Saito, *Chem. Commun.*, 2007, 2133–2135; (h) Y. Taniguchi, Y. Koga, K. Fukabori, R. Kawaguchi and S. Sasaki, *Bioorg. Med. Chem. Lett.*, 2012, **22**, 543–546; (i) T. Ono, S. K. Edwards, S. Wang, W. Jiang and E. T. Kool, *Nucleic Acids Res.*, 2013, **41**, e127; (j) P. Crisalli and E. T. Kool, *Bioconjugate Chem.*, 2011, **22**, 2345–2354.
- 30 (a) S. S. Bag, R. Kundu and S. Jana, *Tetrahedron Lett.*, 2013, **54**, 2627; (b) P. Hazra, D. Chakrabarty, A. Chakraborty and N. Sarkar, *Biochem. Biophys. Res. Commun.*, 2004, **314**, 543; (c) B. K. Paul and N. Guchhait, *J. Phys. Chem. B*, 2011, **115**, 10322.
- 31 S. S. Bag, S. Talukdar and S. K. Das, *Curr. Protoc. Nucleic Acid Chem.*, 2014, **58**, 1.32.1–1.32.27.
- 32 A. Sachin and I. Frank Seela, *Tetrahedron*, 2014, **70**, 380.
- 33 *SMART V 4.043 Software for the CCD Detector System*, Siemens Analytical Instruments Division, Madison, WI, 1995.
- 34 *SAINT V 4.035 Software for the CCD Detector System*, Siemens Analytical Instruments Division, Madison, WI, 1995.
- 35 G. M. Sheldrick, *SHELXL-97, Program for the Refinement of Crystal Structures*, University of Göttingen, Göttingen, Germany, 1997.